Dose-dependent transcriptomic responses of zebrafish eleutheroembryos to Bisphenol A.

Martinez, Ruben; Esteve-Codina, Anna; Herrero-Nogareda, Laia; Ortiz-Villanueva, Elena; Barata, Carlos; Tauler, Roma; Raldua, Demetrio; Pina, Benjamin; Navarro-Martin, Laia

Environmental Pollution, 2018, 243, 988-997

DOI:10.1016/j.envpol.2018.09.043

Dose-dependent transcriptomic responses of zebrafish eleutheroembryos to Bisphenol A

Rubén Martínez[a,b], Anna Esteve-Codina[c,d], Laia Herrero-Nogareda[a], Elena Ortiz-Villanueva[a], Carlos Barata[a], Romà Tauler[a], Demetrio Raldúa[a], Benjamin Piña[a], Laia Navarro-Martín[a*]

[a] Institute of Environmental Assessment and Water Research, IDAEA-CSIC, Barcelona, Catalunya, 08034, Spain

[b] Universitat de Barcelona (UB), Barcelona, Catalunya, 08007, Spain

[c] CNAG-CRG, Centre for Genomic Regulation (CRG), Barcelona Institute of Science and Technology (BIST), Barcelona, Catalunya, 08028, Spain.

[d] Universitat Pompeu Fabra (UPF), Barcelona, Catalunya, 08003, Spain

* Corresponding author: Laia Navarro-Martin, Institute of Environmental Assessment and Water Research, IDAEA-CSIC, Jordi Girona 18, 08034 Barcelona, Spain TEL. +34 93 4006100, ext 1552; E-mail: laianavarromartin@gmail.com

Highlights

· Bisphenol A (BPA) affects steroid, lipid, and visual pathways in zebrafish embryos

· BPA induces persistence of yolk sac remains at 5 dpf and a reduction of eye size

· Transcriptomic changes can be linked with the observed macroscopic alterations

· Transcriptomic effects occur at 1/5 to 1/10 of the macroscopic LOEC

· We propose an interaction of BPA with the estrogen and retinoid regulatory pathways

Graphical Abstract

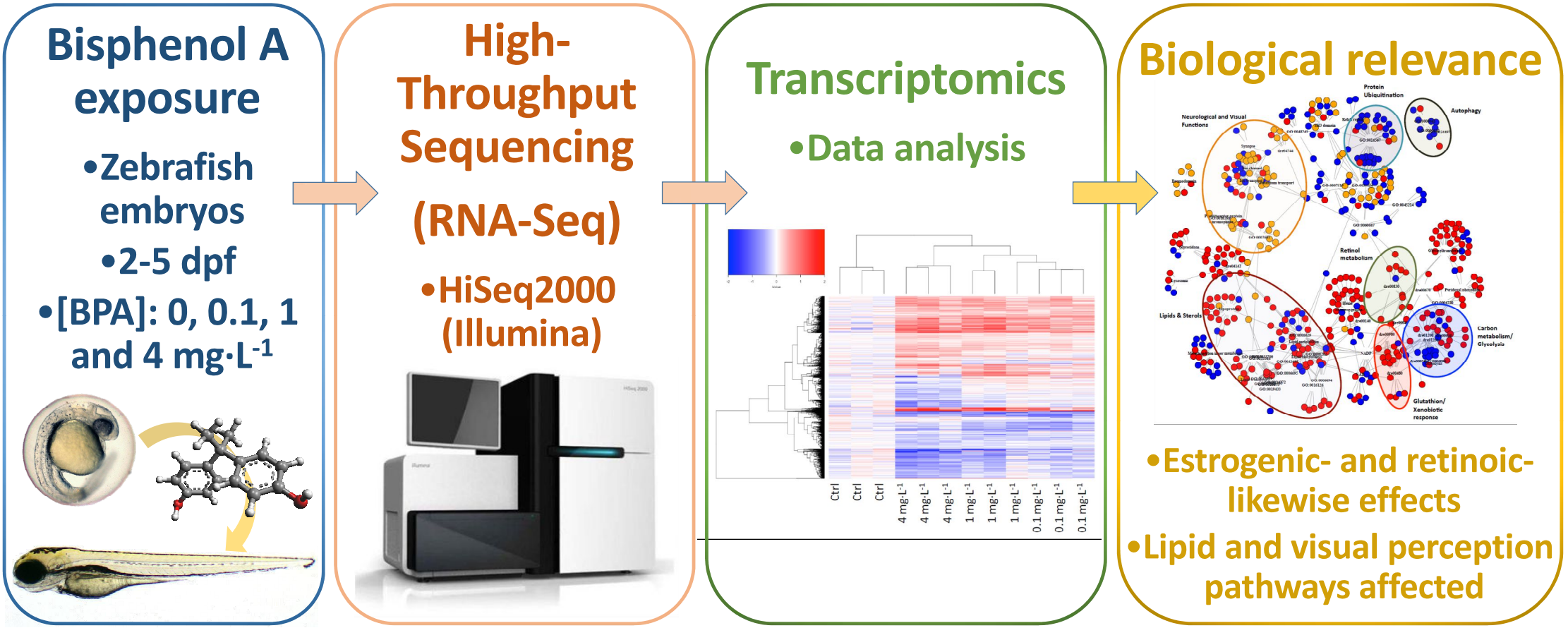

Abstract

Despite the abundant literature on the adverse effects of Bisphenol A (BPA) as endocrine disruptor, its toxicity mechanisms are still poorly understood. We present here a study of its effects on the zebrafish eleutheroembryo transcriptome at concentrations ranging from 0.1 to 4 $mg \cdot L^{-1}$, this latter representing the lowest observed effect concentration (LOEC) found in our study at three different macroscopical endpoints (survival, hatching and swim bladder inflation). Multivariate data analysis methods identified both monotonic and bi-phasic patterns of dose-dependent responses. Functional analyses of genes affected by BPA exposure suggest an interaction of BPA with different signaling pathways, being the estrogenic and retinoid receptors two likely targets. In addition, we identified an apparently unrelated inhibitory effect on, among others, visual function genes. We interpret our data as the result of a sum of underlying, independent molecular mechanisms occurring simultaneously at the exposed animals, well below the macroscopic LOEC, but related to at least some of the observed morphological alterations, particularly in eye size and yolk sac resorption. Our data supports the idea that the physiological effects of BPA cannot be only explained by its rather weak interaction with the estrogen receptor, and that multivariate analyses are required to analyze the effects of toxicants like BPA, which interact with different cellular targets producing complex phenotypes.

Capsule: Estrogenic- and retinoid-like transcriptomic effects of bisphenol A in zebrafish eleutheroembryos and their relationship with morphological alterations.

Keywords: BPA, hormone-response, obesogens, RNA-seq, differentially expressed genes (DEGs), ANOVA-PLS

Introduction

Bisphenol A (BPA) is a key monomer used in the production of certain kind of plastics with wide household uses. It can be found in drink containers, food packaging, adhesives or beverage cans (among many others), as it is amply used in the manufacture of polycarbonate plastics and epoxy resins (Huang et al., 2012; Wang et al., 2015). Many studies have demonstrated that BPA leaks from the original plastics over time, and, as a consequence, it is continuously released in large amounts into the environment. According to the United States Environmental Protection Agency (EPA), the annual release of BPA into the environment exceeded 500 tons in 2012. BPA is ubiquitous in the environment, typically showing parts per billion (ppb) level concentrations in surface waters (from non-detectable to 56.0 $\mu g \cdot L^{-1}$) and plastic items leachates (0.1-7.7 $\mu g \cdot L^{-1}$) (Corrales et al., 2015; Le et al., 2008; Talsness et al., 2009) and parts per million (ppm) levels in landfill leachates (0.001-17.2 $mg \cdot L^{-1}$) and mill effluents (0.0002-0.4 $mg \cdot L^{-1}$) (Canesi and Fabbri, 2015; Flint et al., 2012; Kolpin et al., 2002).

BPA is considered an important threat to the human health, wildlife and environment, owing to its estrogenic activity at environmentally relevant concentrations (0.1-1000 $\mu g \cdot L^{-1}$) (Arase et al., 2011; Cabaton et al., 2011; Careghini et al., 2015; Crain et al., 2007; Kang et al., 2006; Villeneuve et al., 2012; Xu et al., 2013). BPA alters gonadal functions at 0.2 $\mu g \cdot L^{-1}$ - 2.2 $mg \cdot L^{-1}$(Chen et al., 2017; Ekman et al., 2012; Lee et al., 2003; Richter et al., 2007b), and affects hepatic vitellogenin production in fish and other organisms at 0.5-22.8 $mg \cdot L^{-1}$ (Lindholst et al., 2000; Rankouhi et al., 2002). In addition to these effects on reproductive functions, exposure to BPA caused metabolic alterations in different animal models, including disruption of glucose homeostasis in rodents at 10 - 100 µg/kg/day (Alonso-Magdalena et al., 2010), disruption of lipid metabolism, increasing lipid storage and adipogenesis, and affecting body weight later in life at 0.25 - 250 µg/kg/day (Rubin and Soto, 2009; Ryan et al., 2010; Somm et al., 2009). These metabolic effects seem to be related to fundamental cell functions and they have been reported not only in mammals, but also in fish (1.0-4.0 $mg \cdot L^{-1}$) (Ortiz-Villanueva et al., 2017b) and even in crustaceans, like *Daphnia magna* (5.1-32.0 $mg \cdot L^{-1}$) (Jordão et al., 2016b; Nagato et al., 2013). Due to the demonstrated window of sensitivity to BPA exposure during early development, the

European Union and Canadian Authorities have banned the use of BPA in baby bottles and toys. EPA and the European Food Safety Agency (EFSA) established a tolerable daily intake (TDI) of 50 and 4 μg/kg/day, respectively, derived from the no-observed-adverse-effect level (NOAEL) on liver and reproductive toxicity endpoints. This level of exposure, which can be reached from exclusively environmental, non-dietary exposures (EFSA, 2016; Lejonklou et al., 2017), may even be too high to protect consumers and wildlife, as environmentally relevant BPA doses below this TDI are already able to alter reproductive and metabolic functions in exposed animals (Richter et al., 2007a).

Zebrafish (*Danio rerio*) is becoming a preferred model for the analysis of sublethal effects of toxicants in vertebrates (Scholz and Mayer, 2008; Stegeman et al., 2010). It is easy to maintain, it has a short life cycle, and readily produce relatively large quantities of transparent embryos, the development of which has been extensively studied and can be observed using a variety of optical methods. Characteristically, zebrafish embryos hatch only 48-72 hours after fertilization (hpf), continuing its development as free-swimming eleutheroembryos until reaching the larval, self-feeding stage at about 120 hpf (Kimmel et al., 1995; Strähle et al., 2012). Zebrafish has been deeply studied at least at four -*omic* levels: genomics, transcriptomics, proteomics and metabolomics (Mushtaq et al., 2013), and it is considered a convenient vertebrate model for human and environmental toxicology (Raldúa and Piña, 2014; Strähle et al., 2012).

During the last decade, both genomics and transcriptomics have large enhanced their performance specially with the development of high-throughput next generation sequencing (HT-NGS) technologies (Churko et al., 2013; Mortazavi et al., 2008; Reuter et al., 2015). Although both main HT-NGS technologies (microarrays and RNA-seq) have become powerful tools to analyze the transcriptome of many organisms, it has been the last one which has shown better advantages (Wang et al., 2009; Zhao et al., 2014). The use of HT-NGS to examine the effects of endocrine disrupting chemicals (EDCs) in zebrafish is becoming popular (Baker and Hardiman, 2014; Caballero-Gallardo et al., 2016). Nevertheless, most of the studies focus on a reduced dataset of genes, on adult tissues, on a single-dose exposure or on the effects during the first hours when the embryos still haven't developed most organs (Chen et al., 2018; Lam et al., 2011; Renaud et al., 2017; Saili et al., 2013; Tse et al., 2013; Wang et al., 2018).

The aim of the present study was to analyze transcriptome changes in zebrafish eleutheroembryos exposed to BPA and to examine the underlying regulatory mechanisms responsible for the multiple toxic effects of BPA both in aquatic, terrestrial animals and in humans.

Materials and methods

2.1. Animals and rearing conditions

Adult zebrafish (12-18 months old, wild-type *Danio rerio*) were maintained under standard conditions (28 ± 1 °C, 12L:12D photoperiod) and fed twice daily with dry flakes (TetraMin, Tetra, Germany). Eggs were obtained by natural mating and collected and rinsed two hours after fertilization (hpf). Fertilized viable eggs were transferred to fish water (90 μg/ml of Instant Ocean -Aquarium Systems, Sarrebourg, France-, 0.58 mM $CaSO_4 \cdot 2H_2O$, dissolved in reverse osmosis purified water) and kept under standard conditions. All procedures were conducted in accordance with the institutional guidelines under a license from the local government (DAMM 7669, 7964) and were approved by the Institutional Animal Care and Use Committees at the Research and Development Centre of the Spanish Research Council (CID-CSIC).

2.2. Zebrafish eleutheroembryo exposure to BPA

2.2.1. BPA solutions preparation

Bisphenol A (BPA, Sigma-Aldrich, St. Louis, MO, USA) stock solutions (50, 500 and 2000 $mg \cdot L^{-1}$) were prepared in DMSO (dimethyl sulfoxide) and stored at -20 °C. During exposures fresh working solutions were prepared everyday by dissolving the stock solutions in fish water, with a final concentration of DMSO of 0.2% (v/v). Chemical analyses of these solutions were not performed as BPA has been shown to be stable for up to 48 h in water solutions (Jordão et al., 2016b). Preparing and changing water solutions every day until the end of the exposures assured continuous exposure to BPA.

2.2.2. Preliminary range-finding test

A preliminary exposure to BPA concentrations ranging from 0 to 100 mg·L^{-1} was carried out from 2 to 5 days post-fertilization (dpf). During the first 48 h, embryos were kept in clean water to avoid alterations in the very early embryonic process, and to focus in the responses of the already differentiated tissues to BPA. Two dpf embryos were randomly distributed in 6-well microplates at a density of 3 embryos/mL. During the range-finding test, the experimental groups included a vehicle control (0.2% DMSO), 0.1, 1, 2, 4, 6, 8, 10, 50 and 100 mg·L^{-1} BPA. Previous studies done in our laboratory have resulted in 0% survival rates of embryos exposed to environmentally relevant high BPA concentrations (1000 mg·L^{-1}) found in landfill leachate and sewage treatment effluent sources (Crain et al., 2007; Kang et al., 2007). For that reason we set up our experiments to span from 100 mg·L^{-1} to the range of a recent proposed total allowable concentration of BPA for drinking water (100 µg·L^{-1}) (Willhite et al., 2008). For each experimental condition, at least 50 embryos were assessed for survival, hatching, swim bladder inflation rates and sub-lethal and teratogenic effects. Survival (3, 4 and 5 dpf), hatching rates (3, 4 and 5 dpf) and presence of inflated swim bladder (4 and 5 dpf) were recorded for each concentration.

2.2.3. Embryo fixation and morphological traits

Zebrafish eleutheroembryos exposed in the preliminary range-finding test during the period 2-5 dpf were fixed in 4% paraformaldehyde (PFA) in PBS overnight at 4 °C and washed several times with PBS. Fixed eleutheroembryos were gradually transferred to 90% glycerol for preservation and facilitation of eleutheroembryo positioning. Lateral and dorsoventral images of the fixed eleutheroembryos were then taken in order to report morphological effects using a stereomicroscope Nikon SMZ1500 and a Nikon digital Sight DS-Ri1 camera. Embryo standard length, yolk sac area (YSA) and eye size (width) were measured using the free graphical image analysis software ImageJ (National Institutes of Health, Bethesda, MD, USA) (Raldúa et al., 2008). Values (length or width) were normalized by control group mean. Yolk sac area was expressed in mm^2, with baseline correction by subtracting YSA mean value of the control group.

2.2.4. Zebrafish eleutheroembryo exposure to BPA and sample collection

A second experiment was set up to collect samples for transcriptomic analysis. The

concentrations used in the transcriptomic study were chosen to avoid molecular events directly related to alterations in development or embryo viability. In the preliminary range-finding test we determined 4 mg·L^{-1} of BPA as the lowest observed effect concentration (LOEC) (see **section 3.1.**). For that reason, 4 mg·L^{-1} was used as the highest BPA concentration to carry out the exposures for the transcriptomic study. Therefore, eleutheroembryos were exposed to Control (0.2% DMSO), 0.1, 1, and 4 mg·L^{-1} BPA for three days from 2 to 5 dpf. BPA solutions were prepared as indicated above and changed every day. The anatomical development of embryos was followed daily during the exposure (Kimmel et al., 1995). Survival (3, 4 and 5 dpf), hatching rates (3, 4 and 5 dpf) and presence of inflated swim bladder (4 and 5 dpf) were recorded for each concentration. Replicate pools of 10 zebrafish eleutheroembryos were collected per condition from each replicate plate. Samples were snap-frozen in dry ice and stored at -80˚C until further analysis.

2.2.5. Statistical analysis

Differences between treatments in survival, hatching and swim bladder inflation (sections 2.2.2. and 2.2.4.) and in standard length, eye width and yolk sac area (section 2.2.3.) were analyzed using the non-parametric Kruskal-Wallis test with pairwise multiple comparisons since the data did not meet parametric assumptions. Analyses were performed using SPSS 24.0 (Armonk, NY: IBM Corp., 2016). Differences were considered to be significant when $p < 0.05$. Graphs (Figure 1, Supplementary Figures 1 and 2) were performed using GraphPad Prism (v. 6.07, GraphPad Software, La Jolla, CA, USA).

2.3. RNA isolation, library preparation and RNA sequencing

Total RNA was isolated from the pools of 10 whole zebrafish eleutheroembryos using AllPrep DNA/RNA Mini Kit (Qiagen, CA, USA) as described by the manufacturer. Extracted RNA was reconstituted in RNAse-free water. Then, total RNA was assayed for quantity and quality using Qubit® RNA BR Assay kit (Thermo Fisher Scientific) and RNA 6000 Nano Assay on a Bioanalyzer 2100 (Agilent Technologies). Three high-quality RNA biological replicates per condition were sent for sequencing to the National Center for Genomic Analysis (CNAG, Barcelona, Spain). In all cases,

RNA concentrations ranged between 50-200 ng·µL^{-1}, free of DNA and with RNA integrity number (RIN) > 8.

Libraries for RNA-Seq were prepared from total RNA using KAPA Stranded mRNA-Seq Kit Illumina® Platforms (Kapa Biosystems) with minor modifications. Briefly, after poly-A based mRNA enrichment with oligo-dT magnetic beads and 500 ng of total RNA as the input material, the mRNA was fragmented (resulting RNA fragment size was 80-250nt, with the major peak at 130nt). The second strand cDNA synthesis was performed in the presence of dUTP instead of dTTP, to achieve the strand specificity. The blunt-ended double stranded cDNA was 3´adenylated and Illumina indexed adapters (Illumina) were added by ligation. The ligation product was enriched through 15 PCR cycles and the final library was validated on an Agilent 2100 Bioanalyzer with the DNA 7500 assay.

Each library was sequenced using TruSeq SBS Kit v3-HS, in paired-end mode with a read length of 2x76bp. We generated on average 40 million paired-end reads for each sample in a fraction of a sequencing lane on HiSeq2000 (Illumina) following the manufacturer's protocol. Image analysis, base calling and quality scoring of the run were processed using the manufacturer's software Real Time Analysis (RTA 1.13.48) and followed by generation of FASTQ sequence files by CASAVA software. More than 90% of the obtained reads mapped properly to the reference genome. The majority mapped to exonic regions and to protein-coding genes, with a total of 25,000 genes detected per sample.

The data discussed in this publication have been deposited in NCBI's Gene Expression Omnibus (Edgar et al., 2002) and are accessible through GEO Series accession number GSE113676 (https://www.ncbi.nlm.nih.gov/geo/query/acc.cgi?acc=GSE113676). Full description of mapping quality statistics can be found in **Supplementary Table 1**.

2.4. Data processing and differentially expressed genes (DEGs) analysis

RNA-seq reads were aligned to the *D. rerio* reference genome (GRCz10) using STAR version 2.5.1b (Dobin et al., 2013). Genes annotated in GRCz10.84 were quantified using RSEM version 1.2.28 (Li and Dewey, 2011) with default parameters. Data normalization was performed with the DESeq2 (v.1.10.1) R package (Li and Dewey, 2011; Love et al., 2014), which uses a variant of

scaling factor normalization based on the assumption that most genes are not differentially expressed. In our case, we devised a dose-response experiment and decided to analyze both monotonic and non-monotonic responses, as both types of responses have been reported for many endocrine disruptors, including BPA (Vandenberg et al., 2012). For this reason, we chose the supervised ANOVA-PLS (Analysis Of Variance-Partial Least Square) analysis (*lmdme* package in R v. 1.0.136, R Core Team (Fresno et al., 2014)) to perform the differential expression analysis between all experimental conditions. ANOVA decomposes first the data matrix with the transcriptomic information of all samples (normalized and scaled) through a linear model, which takes into account the existence of different levels of exposure to BPA, but without requiring any assumption on the behavior of the different genes among these experimental subsets. In a second step, a PLS regression model is built between the matrices obtained in this linear decomposition (X) and the vector (y) that defines the class membership of the samples (control and BPA treated samples). The analysis determines if the experimental groups are different from each other, and it identifies features (variables) that describe best the differences between groups. We preferred this supervised, multi-level, multivariant method of data analysis as it reflects our experimental setup better than paired tests, like the Student's T test or the PLS-DA (Partial Least Square-Discriminant Analysis), in which a sample (usually, the control) is taken as a reference for all remaining conditions (Fresno et al., 2014). Thereby, ANOVA-PLS was performed on the normalized data scaled to the control set and log2 transformed, considering each one of the BPA concentrations (including controls) as a class. Genes showing significant variations among the classes were selected as DEGs for further analysis. The observed variations in selected DEGs were further confirmed by Real-time qRT-PCR (details presented as supplementary material).

Hierarchical clustering and PAM (partition around medoids) clustering analysis were performed using the packages *gplots*, *fpc*, and *cluster* in R. The PAM implementation in these packages performs a principal component analysis (PCA), to analyze the covariance matrix of the entered variables and to produce a two-dimension plot (two first components) that helps on visualization of how separable the defined clusters were. Samples from each cluster are differentially colored and marked with ellipses

(https://www.rdocumentation.org/packages/cluster/versions/2.0.6/topics/pam). Significant differences between scaled values of all genes included in each cluster were assessed by one-way ANOVA followed by post hoc Tukey's B tests ($p<0.05$) to identify statistically different subsets of samples, using *foreign* and *agricolae* R packages. Further graphs, including heatmaps, were performed with the *gplots* package, also in R.

Functional analysis of DEGs was performed using DAVID Bioinformatic Resources 6.8 Gene enrichment analysis was estimated in DAVID using the default zebrafish (*Danio rerio*) background; enrichment significances were set to a false discovery ratio (FDR) ≤5%. The analysis was limited to GO:Biological Function and KEGG datasets, for simplification. Identified modules with at least five hits were included in the network analysis, using the *reshape2* and *igraph* packages in R (R Development Core Team (2008), 2008). Bipartite graphs were drawn from an incidence table of genes (represented by their official gene names, ZFIN.org), using *igraph*. Any two given genes were considered linked if they share at least one common KEGG or GO (Gene Ontology) module. Metabolic pathways were obtained from the KEGG database.

Results

3.1. Survival hatching and swim bladder (SB) inflation rates

At the end of the preliminary range-finding test no significant differences in survival rates (ranging from 98-100 %) were observed in BPA concentrations up to 10 $mg \cdot L^{-1}$. In contrast survival rates at higher concentrations were found to be 0% (**Supplementary Figure 1**). Gross malformations (**Figure 1**) appeared at BPA concentrations of 10 $mg \cdot L^{-1}$. The first statistically significant effects (Kruskal-Wallis non-parametric test, $p < 0.05$) on hatching and swim bladder (SB) inflation appeared at 8 and 4 $mg \cdot L^{-1}$, respectively. We used the lowest concentration where, at least, one of these parameters was statistically different from the control (4 $mg \cdot L^{-1}$) as the LOEC to perform the next BPA exposure (section 2.2.4.). Similar LOEC value and alterations in development, malformations or larvae viability found in the present study are coincident with previous data (Lam et al., 2011; Ortiz-Villanueva et al., 2017a, 2017b; Pelayo et al., 2012).

During the exposure carried out for the transcriptomic study, mortality was negligible and lethal endpoints such as coagulated embryos, lack of somite formation, non-detachment of the tail, or

lack of heartbeat were not observed. The fraction of non-hatched eggs was only episodic for all concentrations, whereas as expected a significant lower rate of inflated swim bladder was observed at the highest concentration group (4 mg·L^{-1}, Kruskal-Wallis, $p < 0.05$, **Supplementary Figure 2**).

3.2. Analysis of BPA-induced morphological changes

Total embryo length showed a 2-4% reduction at the highest concentration tested that did not presented gross malformations (8 mg·L^{-1}) together with a 10-15% reduction of eye width (**Figure 1**), indicating a mild effect on general embryo development. The most relevant macroscopic effect at this concentration range was the presence of yolk sac remains at 5 dpf, a period at which its resorption by the developing embryo should be essentially complete in normal conditions (**Figures 1A and 1B**). The effect was significant at BPA concentrations above 2 mg·L^{-1} following a linear dose-response effect (**Figures 1A and 1B**).

3.3. Determination and classification of DEGs

The ANOVA-PLS analysis identified 2539 genes differentially expressed in at least one of the experimental subsets (Control, 0.1 mg·L^{-1}, 1 mg·L^{-1}, or 4 mg·L^{-1}) relative to the rest. Hierarchical clustering showed that the expression profiles of the selected DEGs closely reflected the experimental setup, as the different biological replicates for all treatment groups fell into the same hierarchical cluster, except for the 1 mg·L^{-1} class, which appeared divided into two subclusters (**Figure 2**, note that the 0 value -white- corresponds to the averaged control levels). PAM clustering defined three groups of genes, A, B, and C, including 960, 1132 and 447 genes, respectively, corresponding to three different expression patterns among treatment groups (**Figure 3**). Cluster A corresponds to genes whose mRNA levels steadily decreased as the BPA concentration increased, whereas transcripts included in Cluster B showed the opposite behavior. Conversely to the monotonic responses shown in Clusters A and B, genes in Cluster C display a bimodal response, with a maximum in untreated controls, a minimum value at the two middle concentrations, and an intermediate value at 4 mg·L^{-1} (**Figure 3**). **Supplementary Figure**

3 shows a very strong correlation between RNA-seq values and Real Time qRT-PCR estimation of mRNA levels for several selected genes (r^2=0.68, $p \leq 10^{-4}$).

3.4. DEGs Functional characterization

DAVID functional analysis was carried out by both all DEGs together and for each of the three PAM clusters defined in **Figure 3**. Functional modules, either from the GO datasets or from the KEGG dataset with false discovery ratio (FDR) ≤ 5% were selected for further study. **Figure 4A** shows a network representation of modules from both GO:Biological Function and KEGG datasets in which transcripts (dots) are labeled by the cluster they belong; a quantitative representation of the same network is shown in **Figure 4B**. The results show different functional categories particularly enriched in Cluster B (genes upregulated by BPA), which included liver development; lipid transport; lysosome and protein glycosylation; cytochrome P450-mediated metabolism; and different metabolic pathways for lipids, glutathione, retinol, and steroid hormones. Clusters A and C shared most of their principal functional categories, although protein ubiquitination and glycolysis/gluconeogenesis pathways' genes were overrepresented in Cluster A, and Cluster C included a large subset of genes related to visual perception (**Figure 4,** note the colored areas in **Figure 4A**). **Figure 5** shows graphic representations of relative mRNA levels of the genes included in some of these functional modules; the actual output of the DAVID analysis is shown in **Supplementary Table 2**.

3.5. Analysis of putative modes of action of BPA

Comparison between the observed BPA-induced transcriptomic changes with published results of zebrafish eleutheroembryos treated with *all-trans* Retinoic Acid (*at*RA), *9-cis* Retinoic Acid (*9c*RA) (Navarro-Martín et al., 2018), or 17-ß-estradiol (E2) (Hao et al., 2013) revealed similar effects on several functional clusters (**Figure 5**, three bottom lanes). For example, the BPA-induced general up-regulation of genes codifying for the enzymes of the retinol and glutathione metabolic pathways (dre00830 and dre00480, **Figure 5**) was also observed in retinoic acid-treated eleutheroembryos. On the other hand, BPA induced changes in genes typically associated to the estrogenic response, like steroid hormone biosynthesis genes (dre00140), including

cyp19a1b, the brain aromatase (**Figure 5**) (Kishida et al., 2001; Mouriec et al., 2009; Petersen et al., 2013; Puy-Azurmendi et al., 2014). The similarity between BPA- and E2-induced changes extends to at least another functional category, lipid transport (GO:0006869), as three lipid-transport protein genes (*apoa1a, apobb.1, and apoa4a*) showed increased levels of mRNA upon exposure to both BPA and E2 (**Figure 5**). Similar correlations could be also seen, although in a less convincing extend, for the Glucolysis/gluconeogenesis pathway (dre00010). In contrast, the general decrease of visual-perception genes (GO:0007601) was not observed in E2-treated eleutheroembryos, but the same functional cluster showed a general upregulation in both *at*RA and *9c*RA treatments (**Figure 5**).

Discussion

Transcriptome analyses create large datasets that are multivariate in nature, as each gene can be considered as a variable that can be explored to elucidate its relationship with physiological outcomes or with the experimental conditions. These analyses require multivariate analytical tools that reflect the experimental setup, which may vary notably from one experiment to another, depending on the experimental factors that have to be introduced in the model. In our case, we devised a dose-response experiment and decided to analyze both monotonic and non-monotonic responses, as both types of responses have been reported for many endocrine disruptors, including BPA. For this reason, we chose the supervised ANOVA-PLS method (Fresno et al., 2014) as a multivariate analysis that incorporates the existence of different levels of exposure to BPA, but without requiring any assumption on the behavior of the different genes among these experimental subsets. By combining this analysis with the robust, non-supervised PAM clustering, we defined three patterns of expression, two of them reflecting a quasi-linear, monotonic dose-response to BPA, and a third one with a bi-phasic profile. The functional analysis of the genes included in these three clusters revealed that they participate in different biological functions, and that they may reflect the interaction of BPA with different regulatory signals (Murata and Kang, 2018). We observed a strong effect in many metabolic pathways, as shown in **Supplementary Figure 4**. Note that essentially all enzymes involved in testosterone metabolism to estradiol and other steroid hormones became overexpressed upon BPA treatment (**Supp.**

Figure 4A), and so were most of the genes involved in the retinol metabolism (**Supp. Figure 4B**). Those results are coincident with the effects shown by BPA in zebrafish and other animal models (Lam et al., 2011; Lindholst et al., 2000; Morales et al., 2018; Ortiz-Villanueva et al., 2017b; Shmarakov et al., 2017). For the carbon metabolism module (**Suppl. Figure 4C**), there is a clear division between the genes codifying glycolytic enzymes (central pathway), which became downregulated, and those from the pentose-phosphate or the C-1 metabolic pathways, which became mostly upregulated (**Suppl. Figure 4C**).

Most current legal limitations for BPA use in food and baby items are rooted in its alleged estrogenic potency, for which there is abundant information, at least from *in vitro* or *in culture* experiments (Chapin et al., 2008; Vandenberg et al., 2009). This is consistent with the alteration of several estrogen-related genes in BPA-treated samples, including the activation of the brain aromatase, one of the best-known E2-regulated genes in fish embryos, and considered as a specific biomarker of exposure to estrogens (Kishida et al., 2001; Mouriec et al., 2009; Petersen et al., 2013; Puy-Azurmendi et al., 2014). However, most whole-animal toxicological data, either from fish or from mammals, suggest a pleiotropic mode of action that cannot be directly related to BPA estrogenicity (Le Corre et al., 2015; Murata and Kang, 2018; Nishizawa et al., 2003; Wetherill et al., 2007; Zoeller et al., 2005). BPA has profound effects in zebrafish metabolome, affecting lipid, retinol and sugar metabolism (Ortiz-Villanueva et al., 2017a). Our data are consistent with the well-known interaction of BPA with the estrogen receptor, but it also suggests that at least part of the effects observed in BPA treated zebrafish embryo can be explained by the simultaneous activation of other receptors. For example, cytochrome *cyp26* genes become upregulated upon exposure to retinoids (Navarro-Martín et al., 2018), and its activation by BPA strongly suggest an interaction with the retinoic acid and/or the 9-*cis* retinoic acid receptors (RAR, RXR) (Acconcia et al., 2015; Navarro-Martín et al., 2018). The simultaneous activation of both receptors may explain the general upregulation of genes codifying enzymes involved in steroid hormone biosynthesis, glutathione metabolism, or lipid transport, as several of them appear to respond to the presence of one or both effectors. However, some of the observed responses to BPA appear to be unrelated to either estrogen or retinoid pathways, like the simultaneous increase of C1 metabolism and pentose phosphate pathway (PPP) genes, and the

decrease of the glycolytic pathway. These effects may be related to reported BPA-mediated alterations in glucose and lipid homeostasis in mammals, putatively linked to estrogenic effects (Le Corre et al., 2015).

The decrease on different genes related to visual perception can be regarded as the transcriptional counterpart of the observed reduction in eye size. Effects on visual functions have been reported in zebrafish embryos linked to both BPA and bisphenol S, although the underlying mechanism of action is still to be determined (Kinch et al., 2016; Liu et al., 2018; Pelayo et al., 2012). Microphthalmia also was observed in zebrafish eleutheroembryos treated with the thyroid hormone T3, which altered expression of opsin genes (Pelayo et al., 2012), a similar effect, but not identical, to the one observed here. BPA can act as a weak T3 agonist and as potentiator of T3 action, although the very low levels of thyroid function at these specific embryonic stages probably reduce the contribution of this pathway to the observed effects of BPA (Pelayo et al., 2012). It is more likely that the microphthalmia is due to alterations on the retinoid pathway, a key function in early eye development. The bi-modal response to visual perception genes to BPA probably indicates a rather complex toxic interaction, as very low doses of BPA reduced significantly their mRNA levels, an effect that became partially reverted by exposure to the highest tested concentration, which showed a strong inhibitory effect in many metabolic and energy-related transcripts. Exposure to BPA has been related with changes in larvae behavior in light-dark tests (Saili et al., 2012) and with alterations in the ability to discriminate color in adult zebrafish (Li et al., 2017). For that reason, we think that further studies are needed to elucidate if the BPA effects observed in the present study on eye width could be related to vision impairments and in consequence produce alterations in larvae behavioral responses.

Yolk sac resorption appears as a sensitive macroscopic endpoint for embryonic toxicity in zebrafish. Persistence of yolk sac remains beyond 5 dpf has been linked to metabolic alterations in lipid use and energy metabolism in zebrafish (Raldúa et al., 2008; Sant and Timme-Laragy, 2018). Our data suggest that BPA alters both lipid and energy metabolism, by increasing expression of lipid transport-related genes while reducing the expression of the glycolytic pathway. While this suggests a shift from sugar utilization to lipid degradation, it is unclear which

biological mechanism lies behind this effect. Recent reports indicate that a potential candidate is the PPAR/RXR system (Peroxisome Proliferator-Activated Receptor), especially considering the implication of this complex in the regulation of multiple metabolic pathways, and particularly of those related to sugar and lipid metabolism (Huang and Chen, 2017; Lempradl et al., 2015). It is presently unclear whether or not BPA directly interacts with any of the known PPARs, or whether at least part of the effect may be mediated through the co-activator RXR, the 9-*cis* retinoic acid receptor. RXR interacts with many other cellular receptors, and this will at least partially explain the pleiotropic effects of exposure to BPA. For example, this mechanism was suggested to explain the BPA interaction with thyroid hormone regulation, also in zebrafish (Pelayo et al., 2012). In addition, the observed changes produced by BPA in the pattern of energy utilization in zebrafish are reminiscent to the observed accumulation of storage lipids into lipid droplets in the crustacean *D. magna*. As no convincing homolog for PPARs have been found in Crustaceans yet, this effect has been attributed to the putative interaction with RXR and other receptors (Jordão et al., 2016a). Finally, the presence of yolk sac remains at 5 dpf may also be a side effect of the estrogenic activity. E2-treated embryos show at least some of the transcriptomic effects of BPA linked to lipid metabolism (**Figure 5**), and they also show similar macroscopic effects when exposed to high concentrations of E2 (unpublished results). Finally, recent studies using molecular pathway analysis tools suggest multiple effects of BPA on cell signaling, including Fox and MapK pathways in mammals (Murata and Kang, 2018), which could be related to the observed effects on liver, and perhaps also eye, development.

Conclusion

The dose-response setup of our data allows drawing some conclusions about the cause-effect relationship between transcriptomic and morphological responses. While several of the observed changes in transcript abundances can be functionally related to the persistence of yolk sac remains and the shrinkage of eyes, they appeared at exposure levels 5 to 10 fold lower than the observed LOEC for these specific macroscopic alterations (**Figures 1 and 5**). In addition, significant changes on embryo length that could be attributed to a general systemic disruption, only occurred at the highest range of BPA concentrations used in this work (4 $mg \cdot L^{-1}$ and higher). We

therefore consider that the transcriptomic changes are directly related with the primary action of BPA (e.g. receptor interaction or enzyme inhibition) rather than a consequence of the alteration of the embryo development (e.g. changes in tissue formation and composition). We have described transcriptomic alterations reflecting the molecular events implicated in BPA toxicity, which most likely transcend its well-known, but rather weak estrogenic activity. The present study contributes understanding of the environmental and human health hazards associated to the ubiquitous presence of BPA in the environment.

Conflict of interest

The authors declare that they have no conflicts of interest.

Acknowledgments

This work was supported by the European Research Council under the European Union's Seventh Framework Programme (FP/ 2007-2013)/ERC Grant Agreement n. 320737. Some part of this study was also supported by a grant from the Spanish Ministry of Economy and Competitiveness (CTQ2014-56777-R) and by a grant (PT17/0009/0019) from ISCIII (Carlos III Health Institute), part of the Spanish Ministry of Economy and Competitiveness, and cofinanced by the European Regional Development Fund (ERDF). LNM was supported by a Beatriu de Pinos Postdoctoral Fellow (2013BP-B-00088) awarded by the Secretary for Universities and Research of the Ministry of Economy and Knowledge of the Government of Catalonia and the Cofund programme of the Marie Curie Actions of the 7th R&D Framework Programme of the European Union. RM was supported by a FPU predoctoral fellow from the Spanish Ministry of Education and Science (ref. FPU15/03332). We would like to thank Ms. Elia Martinez-Prats and David Angelats for helping with the real time qRT-PCRs measurements.

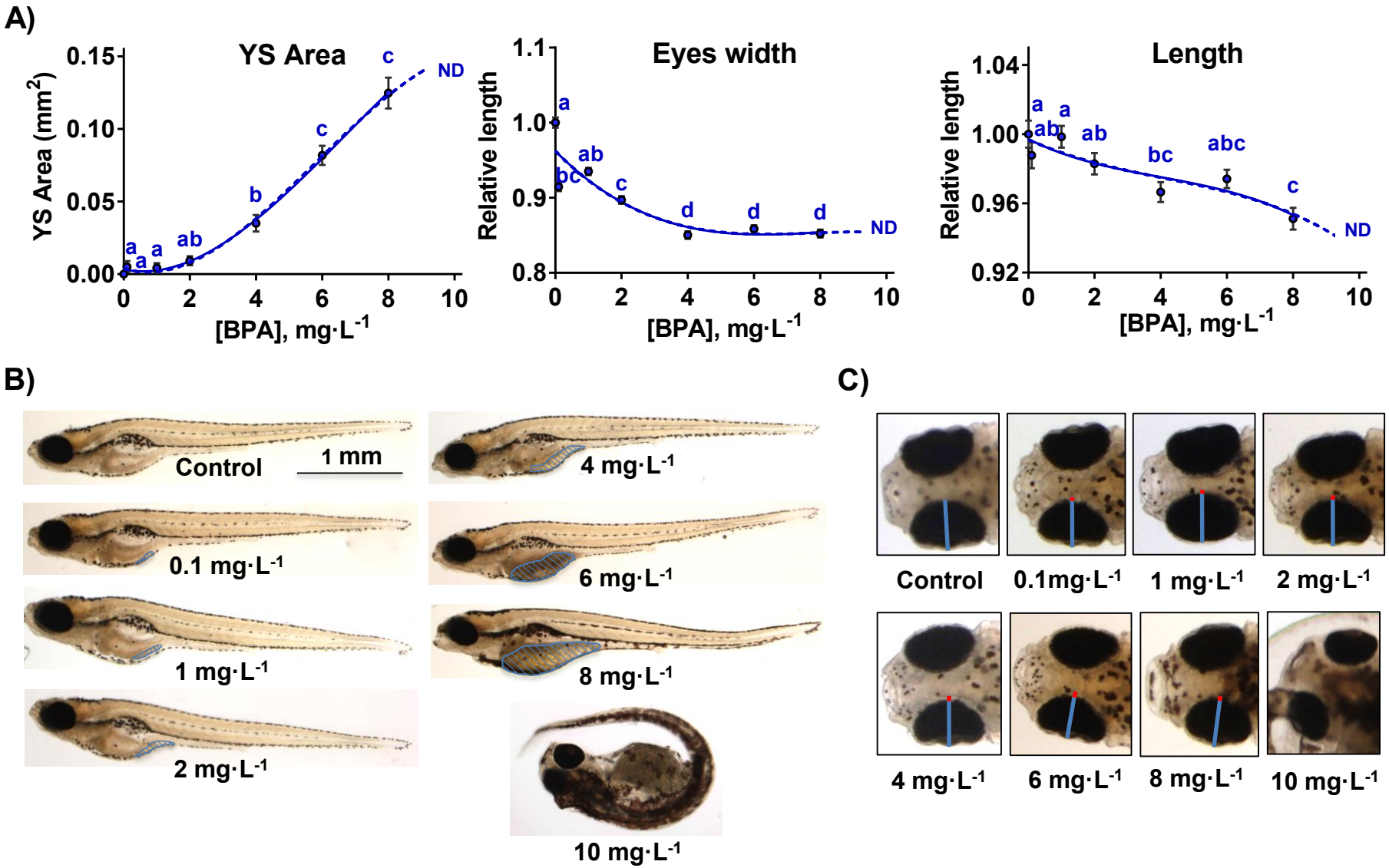
A)
YS Area
YS Area (mm2)
0.15
0.10
0.05
0.00
a
a
a
ab
b
c
c
ND
0
2
4
6
8
10
[BPA], mg·L-1
Eyes width
Relative length
1.1
1.0
0.9
0.8
a
ab
bc
c
d
d
d
ND
[BPA], mg·L-1
Length
Relative length
1.04
1.00
0.96
0.92
a
ab
a
ab
bc
abc
c
ND
[BPA], mg·L-1
B)
Control
1 mm
0.1 mg·L-1
1 mg·L-1
2 mg·L-1
4 mg·L-1
6 mg·L-1
8 mg·L-1
10 mg·L-1
C)
Control
0.1mg·L-1
1 mg·L-1
2 mg·L-1
4 mg·L-1
6 mg·L-1
8 mg·L-1
10 mg·L-1

Figure 1

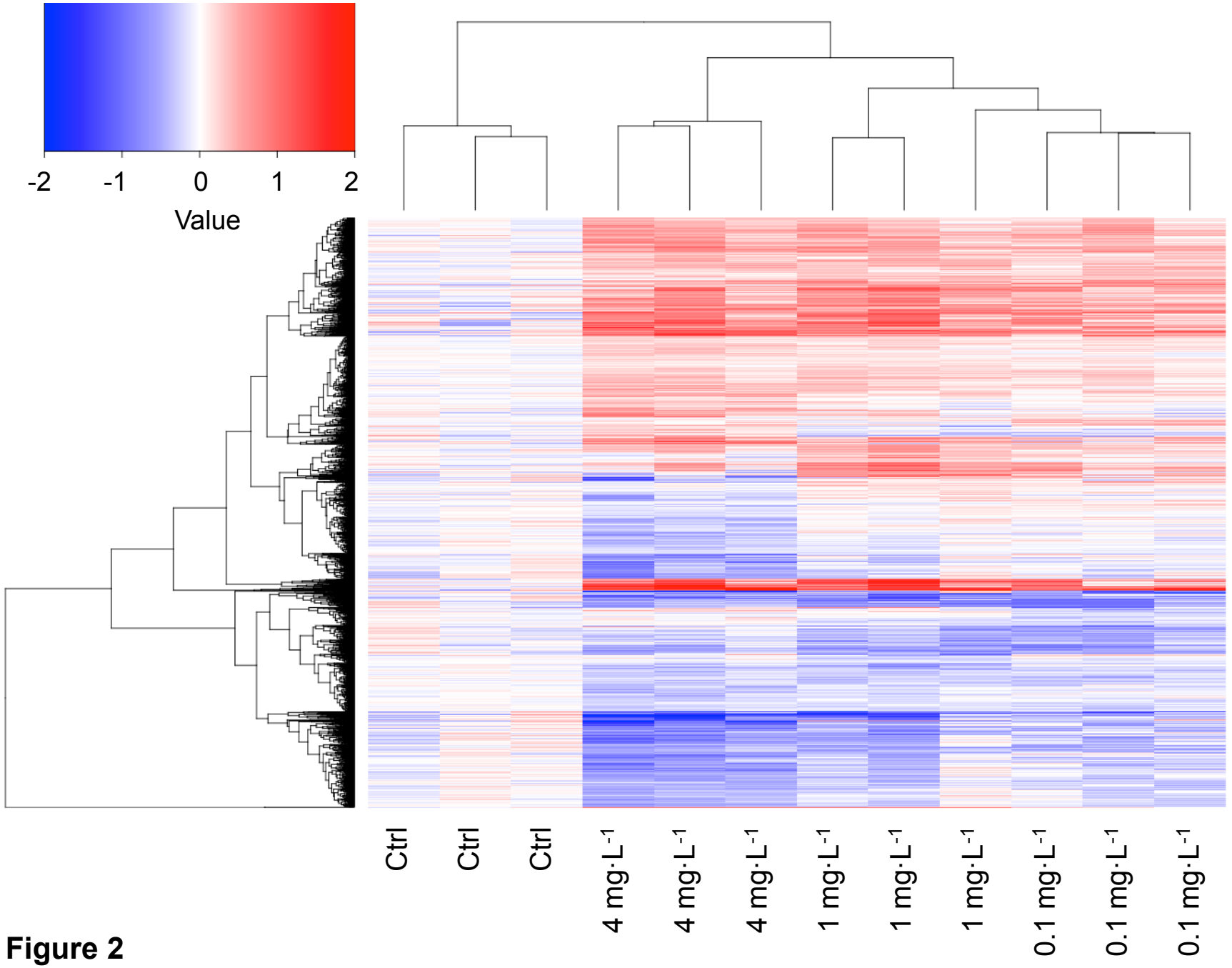
-2
-1
0
1
2
Value
Ctrl
Ctrl
Ctrl
4 mg·L-1
4 mg·L-1
4 mg·L-1
1 mg·L-1
1 mg·L-1
1 mg·L-1
0.1 mg·L-1
0.1 mg·L-1
0.1 mg·L-1

Figure 2

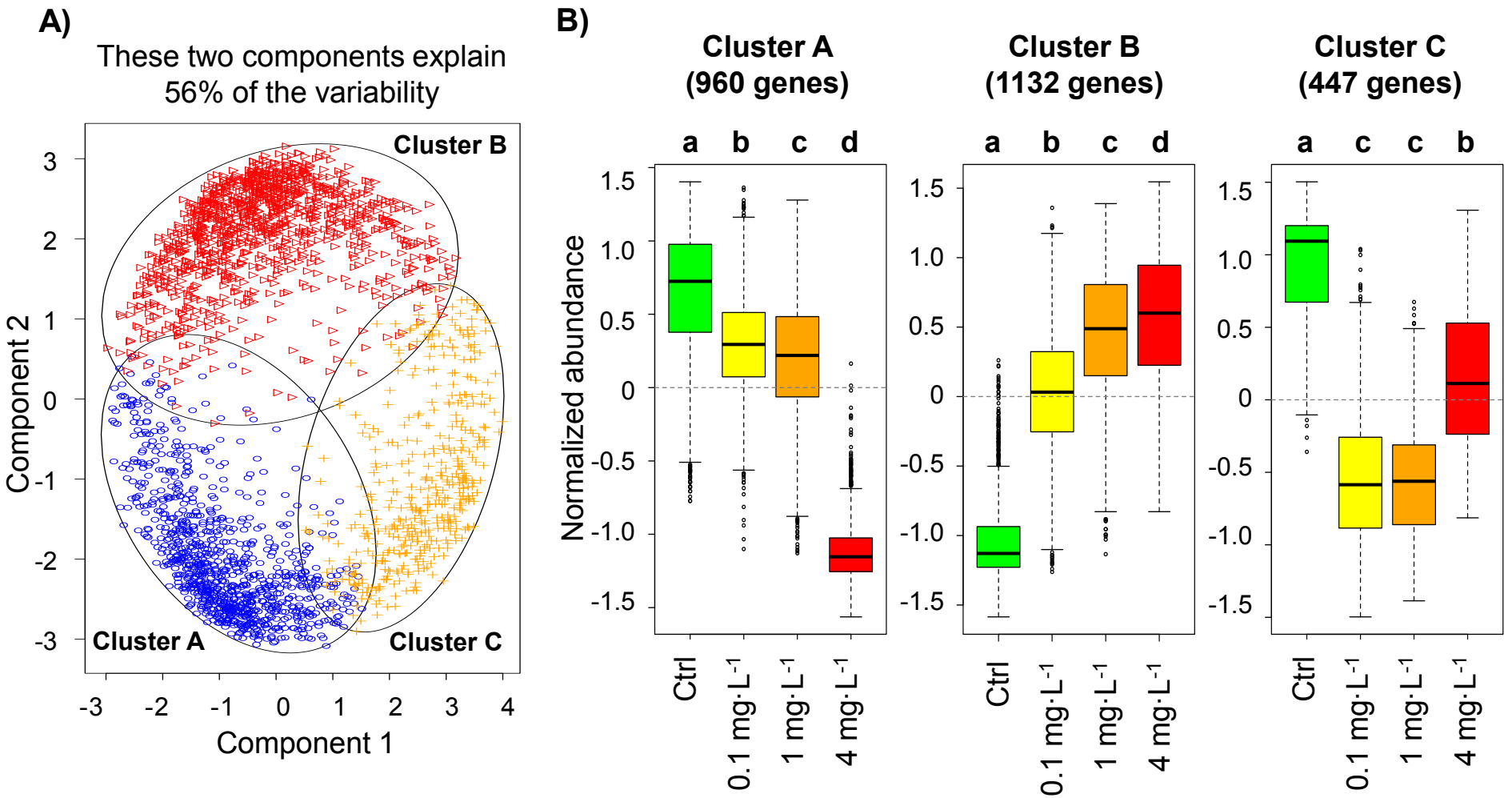
A)
These two components explain
56% of the variability
Cluster B
Cluster A
Cluster C
Component 1
Component 2
B)
Cluster A
(960 genes)
Cluster B
(1132 genes)
Cluster C
(447 genes)
a b c d
a b c d
a c c b
Normalized abundance
Ctrl
0.1 mg·L-1
1 mg·L-1
4 mg·L-1

Figure 3

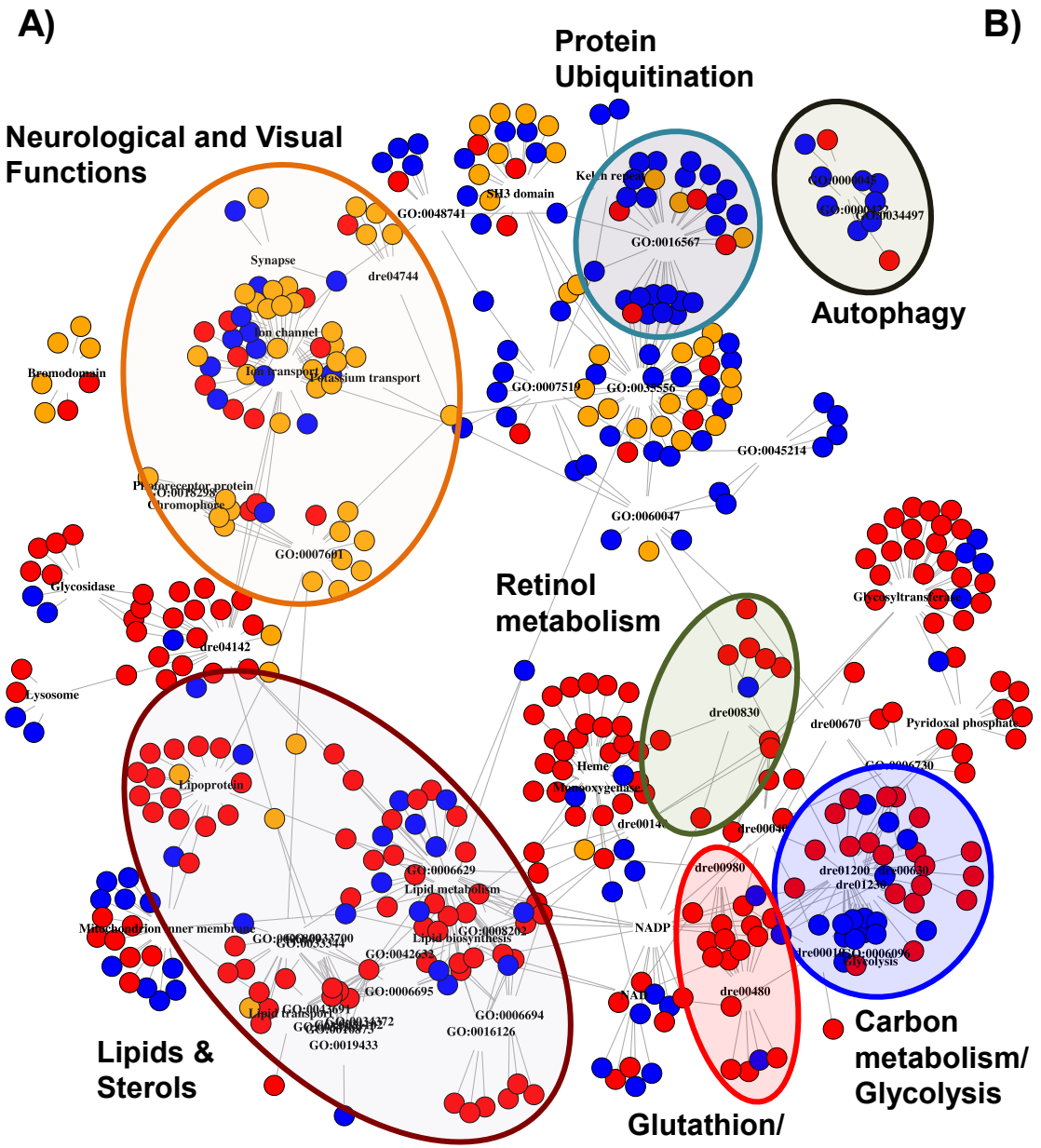

B)

Cluster A	Cluster B	Cluster C	
8	1	0	GO:0000045~autophagosome assembly
8	1	0	Glycolysis
9	1	0	GO:0006096~glycolytic process
7	1	0	GO:0048741~skeletal muscle fiber development
7	1	0	GO:0000422~mitophagy
11	1	0	GO:0007519~skeletal muscle tissue development
10	1	1	GO:0060047~heart contraction
9	1	1	Kelch repeat
7	0	0	GO:0045214~sarcomere organization
5	0	0	GO:0034497~protein localization to pre-autophagosomal structure
11	10	0	dre01230:Biosynthesis of amino acids
12	9	0	Mitochondrion inner membrane
8	7	0	NAD
10	5	0	dre00010:Glycolysis / Gluconeogenesis
24	4	3	GO:0016567~protein ubiquitination
7	4	15	Ion channel
7	3	10	SH3 domain
3	1	8	Synapse
2	1	7	Potassium transport
13	10	18	Ion transport
21	4	18	GO:0035556~intracellular signal transduction
3	22	2	dre04142:Lysosome
4	21	1	Monooxygenase
5	25	0	Glycosyltransferase
3	26	0	Heme
6	14	0	NADP
6	12	0	Lipid biosynthesis
8	19	0	Lipid metabolism
3	10	0	dre00630:Glyoxylate and dicarboxylate metabolism
2	9	0	Glycosidase
1	12	0	dre00480:Glutathione metabolism
2	15	2	Lipoprotein
1	12	2	GO:0006869~lipid transport
11	29	0	GO:0006629~lipid metabolic process
16	17	0	dre01200:Carbon metabolism
0	8	0	dre00140:Steroid hormone biosynthesis
0	8	0	dre00040:Pentose and glucuronate interconversions
0	8	0	dre00830:Retinol metabolism
0	8	0	GO:0006695~cholesterol biosynthetic process
0	8	0	GO:0006730~one-carbon metabolic process
0	7	0	dre00670:One carbon pool by folate
0	10	0	dre00980:Metabolism of xenobiotics by cytochrome P450
0	5	0	GO:0031102~neuron projection regeneration
0	5	0	GO:0010873~positive regulation of cholesterol esterification
0	5	0	GO:0034372~very-low-density lipoprotein particle remodeling
0	5	0	GO:0034380~high-density lipoprotein particle assembly
0	6	0	GO:0043691~reverse cholesterol transport
0	6	0	GO:0042632~cholesterol homeostasis
0	6	1	GO:0033344~cholesterol efflux
0	5	1	GO:0033700~phospholipid efflux
0	9	1	Lipid transport
1	8	0	GO:0008202~steroid metabolic process
1	8	0	GO:0006694~steroid biosynthetic process
1	8	0	Pyridoxal phosphate
1	7	0	GO:0016126~sterol biosynthetic process
1	5	0	GO:0019433~triglyceride catabolic process
2	3	0	dre04142:Lysosome
0	2	5	Bromodomain
0	1	5	dre04744:Phototransduction
0	0	5	GO:0018298~protein-chromophore linkage
0	0	5	Chromophore
0	0	5	Photoreceptor protein
0	1	14	GO:0007601~visual perception

Figure 4

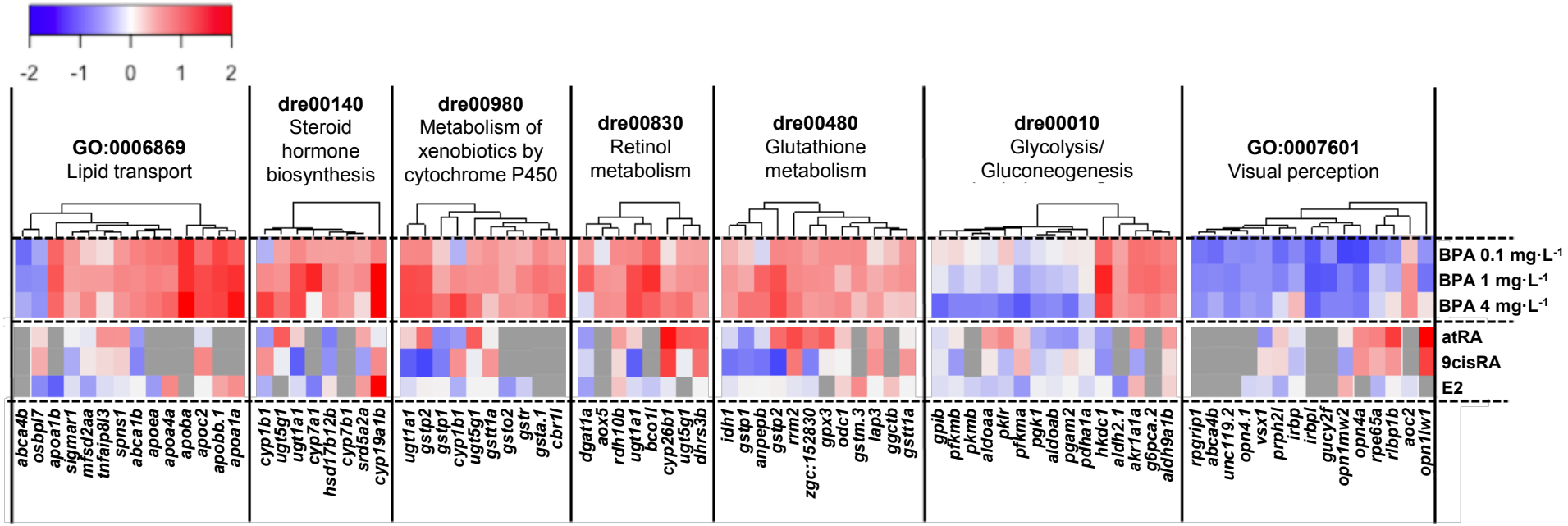
-2
-1
0
1
2
GO:0006869
Lipid transport
dre00140
Steroid hormone biosynthesis
dre00980
Metabolism of xenobiotics by cytochrome P450
dre00830
Retinol metabolism
dre00480
Glutathione metabolism
dre00010
Glycolysis/ Gluconeogenesis
GO:0007601
Visual perception
abca4b
osbpl7
apoa1b
sigmar1
mfsd2aa
tnfaip8l3
spns1
abca1b
apoea
apoa4a
apoba
apoc2
apobb.1
apoa1a
cyp1b1
ugt5g1
ugt1a1
cyp7a1
hsd17b12b
cyp7b1
srd5a2a
cyp19a1b
ugt1a1
gstp2
gstp1
cyp1b1
ugt5g1
gstt1a
gsto2
gstr
gsta.1
cbr1l
dgat1a
aox5
rdh10b
ugt1a1
bco1l
cyp26b1
ugt5g1
dhrs3b
idh1
gstp1
anpepb
gstp2
rrm2
zgc:152830
gpx3
odc1
gstm.3
lap3
ggctb
gstt1a
gpib
pfkmb
pkmb
aldoaa
pklr
pfkma
pgk1
aldoab
pgam2
pdha1a
hkdc1
aldh2.1
akr1a1a
g6pca.2
aldh9a1b
rpgrip1
abca4b
unc119.2
opn4.1
vsx1
prph2l
irbp
irbpl
gucy2f
opn1mw2
opn4a
rpe65a
rlbp1b
aoc2
opn1lw1
BPA 0.1 mg·L-1
BPA 1 mg·L-1
BPA 4 mg·L-1
atRA
9cisRA
E2

Figure 5

Figure Legends

Figure 1. Morphological results from the preliminary range-finding test. **A)** Effects of the BPA exposure in the area of the yolk sac remnants, relative eyes width and relative embryo standard length. The size of the yolk sac (YS Area) is expressed in mm^2, with baseline subtraction. Relative eyes width and standard length is expressed in relative values (normalized by control group mean). Low-case letters in each graph indicate statistically different distributions (Kruskal-Wallis non-parametric test with pairwise multiple comparisons, $p < 0.05$). **B-C)** Representative images of yolk sac area (B) and relative eye width (C) means for each BPA condition are shown. SEM = standard error of the mean. In C), the blue line indicates the length of the control; the red line represents a decrease of that distance. The parameters at 10 $mg \cdot L^{-1}$ were not determined (ND) due to the high rates of malformations at this BPA concentration. Survival rates at 50 and 100 $mg \cdot L^{-1}$ were 0% and in consequence no data exists for both treatment groups.

Figure 2. Heatmap corresponding to 2539 genes identified by ANOVA-PLS as differentially expressed in at least one of the experimental subsets (Control, 0.1 $mg \cdot L^{-1}$, 1 $mg \cdot L^{-1}$, or 4 $mg \cdot L^{-1}$, color bars at the bottom of the map) relative to the rest, hereafter referred to as DEGs, differentially expressed genes. Values were centered to the average of Control samples and then log2 transformed. Color scale ranges from blue (strongly underrepresented relative to controls) to red (strongly overrepresented); white cells correspond to control values. Both rows (genes) and columns (samples) were grouped by hierarchical clustering; the corresponding dendrograms are shown at the left and the top of the panel, respectively.

Figure 3. Results from PAM clustering of DEGs. **A)** PCA analysis showing the three defined clusters labeled in blue, red and yellow (Clusters A, B and C, respectively), as identified by the PAM function in R. The two displayed components explain 56% of total point variability. **B)** Distribution of normalized abundance values for genes included in each of the three clusters. Low-case letters at the top of each graph indicate statistically different distributions (ANOVA + Tukey's B ($p \leq 0.05$) post-hoc test (all possible pairwise comparisons) was used to determine differences between

groups). Thick bars indicate average values, boxes include values between the 1st and 3rd quartiles, whiskers cover the total distribution, except for outliers (circles).

Figure 4. Functional analyses of DEGs, distributed in clusters as shown in Figure 3. **A)** Network representation of DEGs according to their adscription to functional modules (GO:biological process and KEGG databases, codes for each module are given as nodes). DEGs are represented by dots, colored by clusters as in Figure 3. Color areas indicate groups of functional modules considered of particular relevance (see the text). **B)** Distribution of DEGs among the different functional modules (rows) and clusters (columns). Only modules with at least 5 hits in one of the clusters are represented; redundant modules were simplified to the one with the highest number of hits. Numbers indicate the absolute number of DEGs for each module and clusters, colors (heat code, from red -few- to white -most-) represent the relative importance of metabolites associated to each pathway for each cluster; two squares of the same shade of color correspond to identical fraction of DEGs for each cluster.

Figure 5. Graphic representation of mRNA abundance changes of DEGs associated to relevant functional modules, as defined in Figure 4. The three upper rows of each heatmap correspond to relative values for samples treated with 0.1, 1, and 4 $mg \cdot L^{-1}$ BPA (averages of the three biological replicates), respectively. Color scale from blue (underexpression) to red (overexpression) as in Figure 2; note that white represents control values. The three lower rows correspond to microarray data of zebrafish eleutheroembryos treated with either *all-trans* retinoic, *9-cis* retinoic acid [45] or 17-ß-estradiol [46]. Color scale is the same as for BPA-treated samples, although in this case, additional grey sectors correspond to genes not present or not quantified in the corresponding microarray.

References

Acconcia, F., Pallottini, V., Marino, M., 2015. Molecular mechanisms of action of BPA. Dose. Response. 13, 1559325815610582. doi:10.1177/1559325815610582

Alonso-Magdalena, P., Vieira, E., Soriano, S., Menes, L., Burks, D., Quesada, I., Nadal, A., 2010.

Bisphenol A exposure during pregnancy disrupts glucose homeostasis in mothers and adult male offspring. Environ. Health Perspect. 118, 1243–50. doi:10.1289/ehp.1001993

Arase, S., Ishii, K., Igarashi, K., Aisaki, K., Yoshio, Y., Matsushima, A., Shimohigashi, Y., Arima, K., Kanno, J., Sugimura, Y., 2011. Endocrine disrupter bisphenol A increases in situ estrogen production in the mouse urogenital sinus. Biol. Reprod. 84, 734–42. doi:10.1095/biolreprod.110.087502

Baker, M.E., Hardiman, G., 2014. Transcriptional analysis of endocrine disruption using zebrafish and massively parallel sequencing. J. Mol. Endocrinol. 52, R241-56. doi:10.1530/JME-13-0219

Caballero-Gallardo, K., Olivero-Verbel, J., Freeman, J.L., 2016. Toxicogenomics to evaluate endocrine disrupting effects of environmental chemicals using the zebrafish model. Curr. Genomics 17, 515–527. doi:10.2174/1389202917666160513105959

Cabaton, N.J., Wadia, P.R., Rubin, B.S., Zalko, D., Schaeberle, C.M., Askenase, M.H., Gadbois, J.L., Tharp, A.P., Whitt, G.S., Sonnenschein, C., Soto, A.M., 2011. Perinatal exposure to environmentally relevant levels of bisphenol A decreases fertility and fecundity in CD-1 mice. Environ. Health Perspect. 119, 547–52. doi:10.1289/ehp.1002559

Canesi, L., Fabbri, E., 2015. Environmental effects of BPA: focus on aquatic species. Dose. Response. 13, 1559325815598304. doi:10.1177/1559325815598304

Careghini, A., Mastorgio, A.F., Saponaro, S., Sezenna, E., 2015. Bisphenol A, nonylphenols, benzophenones, and benzotriazoles in soils, groundwater, surface water, sediments, and food: a review. Environ. Sci. Pollut. Res. 22, 5711–5741. doi:10.1007/s11356-014-3974-5

Chapin, R.E., Adams, J., Boekelheide, K., Gray, L.E., Hayward, S.W., Lees, P.S.J., McIntyre, B.S., Portier, K.M., Schnorr, T.M., Selevan, S.G., Vandenbergh, J.G., Woskie, S.R., 2008. NTP-CERHR expert panel report on the reproductive and developmental toxicity of bisphenol A. Birth Defects Res. Part B Dev. Reprod. Toxicol. 83, 157–395. doi:10.1002/bdrb.20147

Chen, J., Saili, K.S., Liu, Y., Li, L., Zhao, Y., Jia, Y., Bai, C., Tanguay, R.L., Dong, Q., Huang, C., 2017. Developmental bisphenol A exposure impairs sperm function and reproduction in zebrafish. Chemosphere 169, 262–270. doi:10.1016/j.chemosphere.2016.11.089

Chen, M., Zhang, J., Pang, S., Wang, C., Wang, L., Sun, Y., Song, M., Liang, Y., 2018. Evaluating estrogenic and anti-estrogenic effect of endocrine disrupting chemicals (EDCs) by zebrafish (Danio rerio) embryo-based vitellogenin 1 (vtg1) mRNA expression. Comp. Biochem. Physiol. C. Toxicol. Pharmacol. 204, 45–50. doi:10.1016/j.cbpc.2017.11.010

Churko, J.M., Mantalas, G.L., Snyder, M.P., Wu, J.C., 2013. Overview of high throughput sequencing technologies to elucidate molecular pathways in cardiovascular diseases. Circ. Res. 112, 1613–23. doi:10.1161/CIRCRESAHA.113.300939

Corrales, J., Kristofco, L.A., Steele, W.B., Yates, B.S., Breed, C.S., Williams, E.S., Brooks, B.W., 2015. Global assessment of bisphenol A in the environment: review and analysis of its occurrence and bioaccumulation. Dose. Response. 13, 1559325815598308. doi:10.1177/1559325815598308

Crain, D.A., Eriksen, M., Iguchi, T., Jobling, S., Laufer, H., LeBlanc, G.A., Guillette, L.J., 2007. An ecological assessment of bisphenol-A: evidence from comparative biology. Reprod. Toxicol. 24, 225–239. doi:10.1016/j.reprotox.2007.05.008

Dobin, A., Davis, C.A., Schlesinger, F., Drenkow, J., Zaleski, C., Jha, S., Batut, P., Chaisson, M., Gingeras, T.R., 2013. STAR: ultrafast universal RNA-seq aligner. Bioinformatics 29, 15–21. doi:10.1093/bioinformatics/bts635

EFSA, 2016. Overview of existing methodologies for the estimation of non-dietary exposure to chemicals from the use of consumer products and via the environment. EFSA J. 14, e04525. doi:10.2903/j.efsa.2016.4525

Ekman, D.R., Hartig, P.C., Cardon, M., Skelton, D.M., Teng, Q., Durhan, E.J., Jensen, K.M., Kahl, M.D., Villeneuve, D.L., Gray, L.E., Collette, T.W., Ankley, G.T., 2012. Metabolite profiling and a transcriptional activation assay provide direct evidence of androgen receptor antagonism by bisphenol A in fish. Environ. Sci. Technol. 46, 9673–80. doi:10.1021/es3014634

Flint, S., Markle, T., Thompson, S., Wallace, E., 2012. Bisphenol A exposure, effects, and policy: a wildlife perspective. J. Environ. Manage. 104, 19–34. doi:10.1016/j.jenvman.2012.03.021

Fresno, C., Balzarini, M.G., Fernández, E.A., 2014. lmdme : linear models on designed multivariate experiments in R. J. Stat. Softw. 56. doi:10.18637/jss.v056.i07

Hao, R., Bondesson, M., Singh, A. V., Riu, A., McCollum, C.W., Knudsen, T.B., Gorelick, D.A., Gustafsson, J.-Å., 2013. Identification of estrogen target genes during zebrafish embryonic development through transcriptomic analysis. PLoS One 8, e79020. doi:10.1371/journal.pone.0079020

Huang, Q., Chen, Q., 2017. Mediating roles of PPARs in the effects of environmental chemicals on sex steroids. PPAR Res. 2017, 1–8. doi:10.1155/2017/3203161

Huang, Y.Q., Wong, C.K.C., Zheng, J.S., Bouwman, H., Barra, R., Wahlström, B., Neretin, L., Wong, M.H., 2012. Bisphenol A (BPA) in China: a review of sources, environmental levels, and potential human health impacts. Environ. Int. 42, 91–9. doi:10.1016/j.envint.2011.04.010

Jordão, R., Campos, B., Piña, B., Tauler, R., Soares, A.M.V.M., Barata, C., 2016a. Mechanisms of action of compounds that enhance storage lipid accumulation in Daphnia magna. Environ. Sci. Technol. 50, 13565–13573. doi:10.1021/acs.est.6b04768

Jordão, R., Garreta, E., Campos, B., Lemos, M.F.L., Soares, A.M.V.M., Tauler, R., Barata, C., 2016b. Compounds altering fat storage in Daphnia magna. Sci. Total Environ. 545–546, 127–136. doi:10.1016/j.scitotenv.2015.12.097

Kang, J.-H., Asai, D., Aasi, D., Katayama, Y., 2007. Bisphenol A in the aquatic environment and its endocrine-disruptive effects on aquatic organisms. Crit. Rev. Toxicol. 37, 607–25. doi:10.1080/10408440701493103

Kang, J.-H., Kondo, F., Katayama, Y., 2006. Human exposure to bisphenol A. Toxicology 226, 79–89. doi:10.1016/j.tox.2006.06.009

Kimmel, C.B., Ballard, W.W., Kimmel, S.R., Ullmann, B., Schilling, T.F., 1995. Stages of embryonic development of the zebrafish. Dev. Dyn. 203, 253–310. doi:10.1002/aja.1002030302

Kinch, C.D., Kurrasch, D.M., Habibi, H.R., 2016. Adverse morphological development in embryonic zebrafish exposed to environmental concentrations of contaminants individually and in mixture. Aquat. Toxicol. 175, 286–298. doi:10.1016/j.aquatox.2016.03.021

Kishida, M., McLellan, M., Miranda, J.A., Callard, G. V., 2001. Estrogen and xenoestrogens upregulate the brain aromatase isoform (P450aromB) and perturb markers of early development in zebrafish (Danio rerio). Comp. Biochem. Physiol. Part B Biochem. Mol. Biol. 129, 261–268. doi:10.1016/S1096-4959(01)00319-0

Kolpin, D.W., Furlong, E.T., Meyer, M.T., Thurman, E.M., Zaugg, S.D., Barber, L.B., Buxton, H.T., 2002. Pharmaceuticals, hormones, and other organic wastewater contaminants in U.S. streams, 1999-2000: a national reconnaissance. Environ. Sci. Technol. 36, 1202–11. doi:10.1021/es011055j

Lam, S.H., Hlaing, M.M., Zhang, X., Yan, C., Duan, Z., Zhu, L., Ung, C.Y., Mathavan, S., Ong, C.N., Gong, Z., 2011. Toxicogenomic and phenotypic analyses of bisphenol-a early-life exposure toxicity in zebrafish. PLoS One 6. doi:10.1371/journal.pone.0028273

Le, H.H., Carlson, E.M., Chua, J.P., Belcher, S.M., 2008. Bisphenol A is released from polycarbonate drinking bottles and mimics the neurotoxic actions of estrogen in developing cerebellar neurons. Toxicol. Lett. 176, 149–156. doi:10.1016/j.toxlet.2007.11.001

Le Corre, L., Besnard, P., Chagnon, M.-C., 2015. BPA, an energy balance disruptor. Crit. Rev. Food Sci. Nutr. 55, 769–77. doi:10.1080/10408398.2012.678421

Lee, H.J., Chattopadhyay, S., Gong, E.-Y., Ahn, R.S., Lee, K., 2003. Antiandrogenic effects of bisphenol A and nonylphenol on the function of androgen receptor. Toxicol. Sci. 75, 40–6. doi:10.1093/toxsci/kfg150

Lejonklou, M.H., Dunder, L., Bladin, E., Pettersson, V., Rönn, M., Lind, L., Waldén, T.B., Lind, P.M., 2017. Effects of low-dose developmental bisphenol A exposure on metabolic parameters and gene expression in male and female Fischer 344 rat offspring. Environ. Health Perspect. 125, 67018. doi:10.1289/EHP505

Lempradl, A., Pospisilik, J.A., Penninger, J.M., 2015. Exploring the emerging complexity in transcriptional regulation of energy homeostasis. Nat. Rev. Genet. 16, 665–681. doi:10.1038/nrg3941

Li, B., Dewey, C.N., 2011. RSEM: accurate transcript quantification from RNA-Seq data with or without a reference genome. BMC Bioinformatics 12, 323. doi:10.1186/1471-2105-12-323

Li, X., Sun, M.-Z., Li, X., Zhang, S.-H., Dai, L.-T., Liu, X.-Y., Zhao, X., Chen, D.-Y., Feng, X.-Z., 2017. Impact of low-dose chronic exposure to Bisphenol A (BPA) on adult male zebrafish adaption to the environmental complexity: Disturbing the color preference patterns and reliving the anxiety behavior. Chemosphere 186, 295–304.

doi:10.1016/j.chemosphere.2017.07.164

Lindholst, C., Pedersen, K.L., Pedersen, S.N., 2000. Estrogenic response of bisphenol A in rainbow trout (Oncorhynchus mykiss). Aquat. Toxicol. 48, 87–94. doi:10.1016/S0166-445X(99)00051-X

Liu, W., Zhang, X., Wei, P., Tian, H., Wang, W., Ru, S., 2018. Long-term exposure to bisphenol S damages the visual system and reduces the tracking capability of male zebrafish (Danio rerio). J. Appl. Toxicol. 38, 248–258. doi:10.1002/jat.3519

Love, M.I., Huber, W., Anders, S., 2014. Moderated estimation of fold change and dispersion for RNA-seq data with DESeq2. Genome Biol. 15, 550. doi:10.1186/s13059-014-0550-8

Morales, M., Martínez-Paz, P., Sánchez-Argüello, P., Morcillo, G., Martínez-Guitarte, J.L., 2018. Bisphenol A (BPA) modulates the expression of endocrine and stress response genes in the freshwater snail Physa acuta. Ecotoxicol. Environ. Saf. 152, 132–138. doi:10.1016/j.ecoenv.2018.01.034

Mortazavi, A., Williams, B.A., McCue, K., Schaeffer, L., Wold, B., 2008. Mapping and quantifying mammalian transcriptomes by RNA-Seq. Nat. Methods 5, 621–628. doi:10.1038/nmeth.1226

Mouriec, K., Lareyre, J.J., Tong, S.K., Le Page, Y., Vaillant, C., Pellegrini, E., Pakdel, F., Chung, B.C., Kah, O., Anglade, I., 2009. Early regulation of brain aromatase (cyp19a1b) by estrogen receptors during zebrafish development. Dev. Dyn. 238, 2641–2651. doi:10.1002/dvdy.22069

Murata, M., Kang, J.-H., 2018. Bisphenol A (BPA) and cell signaling pathways. Biotechnol. Adv. 36, 311–327. doi:10.1016/j.biotechadv.2017.12.002

Mushtaq, M.Y., Verpoorte, R., Kim, H.K., 2013. Zebrafish as a model for systems biology. Biotechnol. Genet. Eng. Rev. 29, 187–205. doi:10.1080/02648725.2013.801238

Nagato, E.G., D'eon, J.C., Lankadurai, B.P., Poirier, D.G., Reiner, E.J., Simpson, A.J., Simpson, M.J., 2013. (1)H NMR-based metabolomics investigation of Daphnia magna responses to sub-lethal exposure to arsenic, copper and lithium. Chemosphere 93, 331–7. doi:10.1016/j.chemosphere.2013.04.085

Navarro-Martín, L., Oliveira, E., Casado, M., Barata, C., Piña, B., 2018. Dysregulatory effects of retinoic acid isomers in late zebrafish embryos. Environ. Sci. Pollut. Res. 25, 3849–3859. doi:10.1007/s11356-017-0732-5

Nishizawa, H., Manabe, N., Morita, M., Sugimoto, M., Imanishi, S., Miyamoto, H., 2003. Effects of in utero exposure to bisphenol A on expression of RARalpha and RXRalpha mRNAs in murine embryos. J. Reprod. Dev. 49, 539–45.

Ortiz-Villanueva, E., Benavente, F., Piña, B., Sanz-Nebot, V., Tauler, R., Jaumot, J., 2017a. Knowledge integration strategies for untargeted metabolomics based on MCR-ALS analysis of CE-MS and LC-MS data. Anal. Chim. Acta 978, 10–23. doi:10.1016/j.aca.2017.04.049

Ortiz-Villanueva, E., Navarro-Martín, L., Jaumot, J., Benavente, F., Sanz-Nebot, V., Piña, B.,

Tauler, R., 2017b. Metabolic disruption of zebrafish (Danio rerio) embryos by bisphenol A. An integrated metabolomic and transcriptomic approach. Environ. Pollut. 231, 22–36. doi:10.1016/j.envpol.2017.07.095

Pelayo, S., Oliveira, E., Thienpont, B., Babin, P.J., Raldúa, D., André, M., Piña, B., 2012. Triiodothyronine-induced changes in the zebrafish transcriptome during the eleutheroembryonic stage: Implications for bisphenol A developmental toxicity. Aquat. Toxicol. 110–111, 114–122. doi:10.1016/j.aquatox.2011.12.016

Petersen, K., Fetter, E., Kah, O., Brion, F., Scholz, S., Tollefsen, K.E., 2013. Transgenic (cyp19a1b-GFP) zebrafish embryos as a tool for assessing combined effects of oestrogenic chemicals. Aquat. Toxicol. 138–139, 88–97. doi:10.1016/j.aquatox.2013.05.001

Puy-Azurmendi, E., Olivares, A., Vallejo, A., Ortiz-Zarragoitia, M., Piña, B., Zuloaga, O., Cajaraville, M.P., 2014. Estrogenic effects of nonylphenol and octylphenol isomers in vitro by recombinant yeast assay (RYA) and in vivo with early life stages of zebrafish. Sci. Total Environ. 466–467, 1–10. doi:10.1016/j.scitotenv.2013.06.060

R Development Core Team (2008), 2008. R: a language and environment for statistical computing, R Foundation for Statistical Computing.

Raldúa, D., André, M., Babin, P.J., 2008. Clofibrate and gemfibrozil induce an embryonic malabsorption syndrome in zebrafish. Toxicol. Appl. Pharmacol. 228, 301–314. doi:10.1016/j.taap.2007.11.016

Raldúa, D., Piña, B., 2014. In vivo zebrafish assays for analyzing drug toxicity. Expert Opin. Drug Metab. Toxicol. 10, 685–697. doi:10.1517/17425255.2014.896339

Rankouhi, T.R., van Holsteijn, I., Letcher, R., Giesy, J.P., van Den Berg, M., 2002. Effects of primary exposure to environmental and natural estrogens on vitellogenin production in carp (Cyprinus carpio) hepatocytes. Toxicol. Sci. 67, 75–80. doi:10.1093/toxsci/67.1.75

Renaud, L., Silveira, W.A. da, Hazard, E.S., Simpson, J., Falcinelli, S., Chung, D., Carnevali, O., Hardiman, G., 2017. The plasticizer bisphenol A perturbs the hepatic epigenome: a systems level analysis of the miRNome. Genes (Basel). 8, 269. doi:10.3390/genes8100269

Reuter, J.A., Spacek, D. V., Snyder, M.P., 2015. High-Throughput Sequencing Technologies. Mol. Cell. doi:10.1016/j.molcel.2015.05.004

Richter, C.A., Birnbaum, L.S., Farabollini, F., Newbold, R.R., Rubin, B.S., Talsness, C.E., Vandenbergh, J.G., Walser-Kuntz, D.R., vom Saal, F.S., 2007a. In vivo effects of bisphenol A in laboratory rodent studies. Reprod. Toxicol. 24, 199–224. doi:10.1016/j.reprotox.2007.06.004

Richter, C.A., Taylor, J.A., Ruhlen, R.L., Welshons, W. V., Vom Saal, F.S., 2007b. Estradiol and Bisphenol A stimulate androgen receptor and estrogen receptor gene expression in fetal mouse prostate mesenchyme cells. Environ. Health Perspect. 115, 902–8. doi:10.1289/ehp.9804

Rubin, B.S., Soto, A.M., 2009. Bisphenol A: Perinatal exposure and body weight. Mol. Cell. Endocrinol. 304, 55–62. doi:10.1016/j.mce.2009.02.023

Ryan, K.K., Haller, A.M., Sorrell, J.E., Woods, S.C., Jandacek, R.J., Seeley, R.J., 2010. Perinatal exposure to bisphenol-a and the development of metabolic syndrome in CD-1 mice. Endocrinology 151, 2603–12. doi:10.1210/en.2009-1218

Saili, K.S., Corvi, M.M., Weber, D.N., Patel, A.U., Das, S.R., Przybyla, J., Anderson, K.A., Tanguay, R.L., 2012. Neurodevelopmental low-dose bisphenol A exposure leads to early life-stage hyperactivity and learning deficits in adult zebrafish. Toxicology 291, 83–92. doi:10.1016/j.tox.2011.11.001

Saili, K.S., Tilton, S.C., Waters, K.M., Tanguay, R.L., 2013. Global gene expression analysis reveals pathway differences between teratogenic and non-teratogenic exposure concentrations of bisphenol A and 17β-estradiol in embryonic zebrafish. Reprod. Toxicol. 38, 89–101. doi:10.1016/j.reprotox.2013.03.009

Sant, K.E., Timme-Laragy, A.R., 2018. Zebrafish as a model for toxicological perturbation of yolk and nutrition in the early embryo. Curr. Environ. Heal. reports 5, 125–133. doi:10.1007/s40572-018-0183-2

Scholz, S., Mayer, I., 2008. Molecular biomarkers of endocrine disruption in small model fish. Mol. Cell. Endocrinol. 293, 57–70. doi:10.1016/j.mce.2008.06.008

Shmarakov, I.O., Borschovetska, V.L., Blaner, W.S., 2017. Hepatic detoxification of bisphenol A is retinoid-dependent. Toxicol. Sci. 157, 141–155. doi:10.1093/toxsci/kfx022

Somm, E., Schwitzgebel, V.M., Toulotte, A., Cederroth, C.R., Combescure, C., Nef, S., Aubert, M.L., Hüppi, P.S., 2009. Perinatal exposure to bisphenol a alters early adipogenesis in the rat. Environ. Health Perspect. 117, 1549–55. doi:10.1289/ehp.11342

Stegeman, J.J., Goldstone, J. V, Hahn, M.E., 2010. Perspectives on zebrafish as a model in environmental toxicology, in: Zebrafish Volume 29. pp. 367–439. doi:10.1016/S1546-5098(10)02910-9

Strähle, U., Scholz, S., Geisler, R., Greiner, P., Hollert, H., Rastegar, S., Schumacher, A., Selderslaghs, I., Weiss, C., Witters, H., Braunbeck, T., 2012. Zebrafish embryos as an alternative to animal experiments—A commentary on the definition of the onset of protected life stages in animal welfare regulations. Reprod. Toxicol. 33, 128–132. doi:10.1016/j.reprotox.2011.06.121

Talsness, C.E., Andrade, A.J.M., Kuriyama, S.N., Taylor, J.A., vom Saal, F.S., 2009. Components of plastic: experimental studies in animals and relevance for human health. Philos. Trans. R. Soc. B Biol. Sci. 364, 2079–2096. doi:10.1098/rstb.2008.0281

Tse, W.K.F., Yeung, B.H.Y., Wan, H.T., Wong, C.K.C., 2013. Early embryogenesis in zebrafish is affected by bisphenol A exposure. Biol. Open 2, 466–71. doi:10.1242/bio.20134283

Vandenberg, L.N., Colborn, T., Hayes, T.B., Heindel, J.J., Jacobs, D.R., Lee, D.-H., Shioda, T., Soto, A.M., vom Saal, F.S., Welshons, W. V., Zoeller, R.T., Myers, J.P., 2012. Hormones and endocrine-disrupting chemicals: low-dose effects and nonmonotonic dose responses. Endocr. Rev. 33, 378–455. doi:10.1210/er.2011-1050

Vandenberg, L.N., Maffini, M. V., Sonnenschein, C., Rubin, B.S., Soto, A.M., 2009. Bisphenol-A

and the great divide: a review of controversies in the field of endocrine disruption. Endocr. Rev. 30, 75–95. doi:10.1210/er.2008-0021

Villeneuve, D.L., Garcia-Reyero, N., Escalon, B.L., Jensen, K.M., Cavallin, J.E., Makynen, E.A., Durhan, E.J., Kahl, M.D., Thomas, L.M., Perkins, E.J., Ankley, G.T., 2012. Ecotoxicogenomics to support ecological risk assessment: a case study with bisphenol A in fish. Environ. Sci. Technol. 46, 51–9. doi:10.1021/es201150a

Wang, P., Xia, P., Yang, J., Wang, Z., Peng, Y., Shi, W., Villeneuve, D.L., Yu, H., Zhang, X., 2018. A reduced transcriptome approach to assess environmental toxicants using zebrafish embryo test. Environ. Sci. Technol. 52, 821–830. doi:10.1021/acs.est.7b04073

Wang, S., Wang, L., Hua, W., Zhou, M., Wang, Q., Zhou, Q., Huang, X., 2015. Effects of bisphenol A, an environmental endocrine disruptor, on the endogenous hormones of plants. Environ. Sci. Pollut. Res. 22, 17653–17662. doi:10.1007/s11356-015-4972-y

Wang, Z., Gerstein, M., Snyder, M., 2009. RNA-Seq: a revolutionary tool for transcriptomics. Nat. Rev. Genet. 10, 57–63. doi:10.1038/nrg2484

Wetherill, Y.B., Akingbemi, B.T., Kanno, J., McLachlan, J.A., Nadal, A., Sonnenschein, C., Watson, C.S., Zoeller, R.T., Belcher, S.M., 2007. In vitro molecular mechanisms of bisphenol A action. Reprod. Toxicol. 24, 178–198. doi:10.1016/j.reprotox.2007.05.010

Willhite, C.C., Ball, G.L., McLellan, C.J., 2008. Derivation of a bisphenol A oral reference dose (RfD) and drinking-water equivalent concentration. J. Toxicol. Environ. Heal. Part B 11, 69–146. doi:10.1080/10937400701724303

Xu, H., Yang, M., Qiu, W., Pan, C., Wu, M., 2013. The impact of endocrine-disrupting chemicals on oxidative stress and innate immune response in zebrafish embryos. Environ. Toxicol. Chem. 32, 1793–1799. doi:10.1002/etc.2245

Zhao, S., Fung-Leung, W.-P., Bittner, A., Ngo, K., Liu, X., 2014. Comparison of RNA-Seq and microarray in transcriptome profiling of activated T cells. PLoS One 9, e78644. doi:10.1371/journal.pone.0078644

Zoeller, R.T., Bansal, R., Parris, C., 2005. Bisphenol-A, an environmental contaminant that acts as a thyroid hormone receptor antagonist in vitro, increases serum thyroxine, and alters RC3/neurogranin expression in the developing rat brain. Endocrinology 146, 607–12. doi:10.1210/en.2004-1018

Supplementary Material

Supplementary Methods

RT-qPCR analysis

RNA subsamples from the different preparations used for RNA seq were reverse-transcribed to cDNA using Transcriptor First Strand cDNa Sythesis Kit (Roche Diagnostics) following manufacturer's protocols. Eight transcripts were analyzed, *ppiaa* (reference gene)*, aldoab, apoba1, cyp19a1b, fads2, gsta.1, pklr,* and *rpe65a.* Primers were designed using Primer Express 2.0 software (Applied Biosystems, Foster City, CA, USA) and the Primer-Blast server (http://www.ncbi.nlm.nih.gov/ Tools / primer-blast) and synthesized by Sigma (San Louis, MO, USA, final primer pairs are listed in **Supplementary Table 3**). Real-time PCR reactions were carried out on LightCycler® 480 Real-Time PCR System (Roche Diagnostics, Mannheim, Germany). The amplification program used consisted of 10 min at 95 °C, followed by 45 cycles (10 s at 95 °C, 30 s at 60 °C). After the amplification, a dissociation analysis was also programmed to evaluate the specificity of the reaction.

The efficiency of amplification reaction of each target gene was evaluated by serial dilutions of cDNA and subjected to amplification under the same conditions as above. Relative mRNA abundances of different genes were calculated from the second derivative maximum of their respective amplification curves (Cp, calculated by duplicates). To minimize errors in RNA quantification among different samples, Cp values for target genes (Cptg) were normalized to the average Cp values of reference gene, following the equation: ΔCptg = Cpppiaa – Cptg. Changes in mRNA abundance in samples from different treatments were calculated by the ΔΔCp method (Pfaffl, 2001), using corrected Cp values from treated and non-treated samples, following the equation: ΔΔCptg = ΔCptg_untreated − ΔCptg_treated. Fold-change ratios were derived from those ΔΔCptg values.

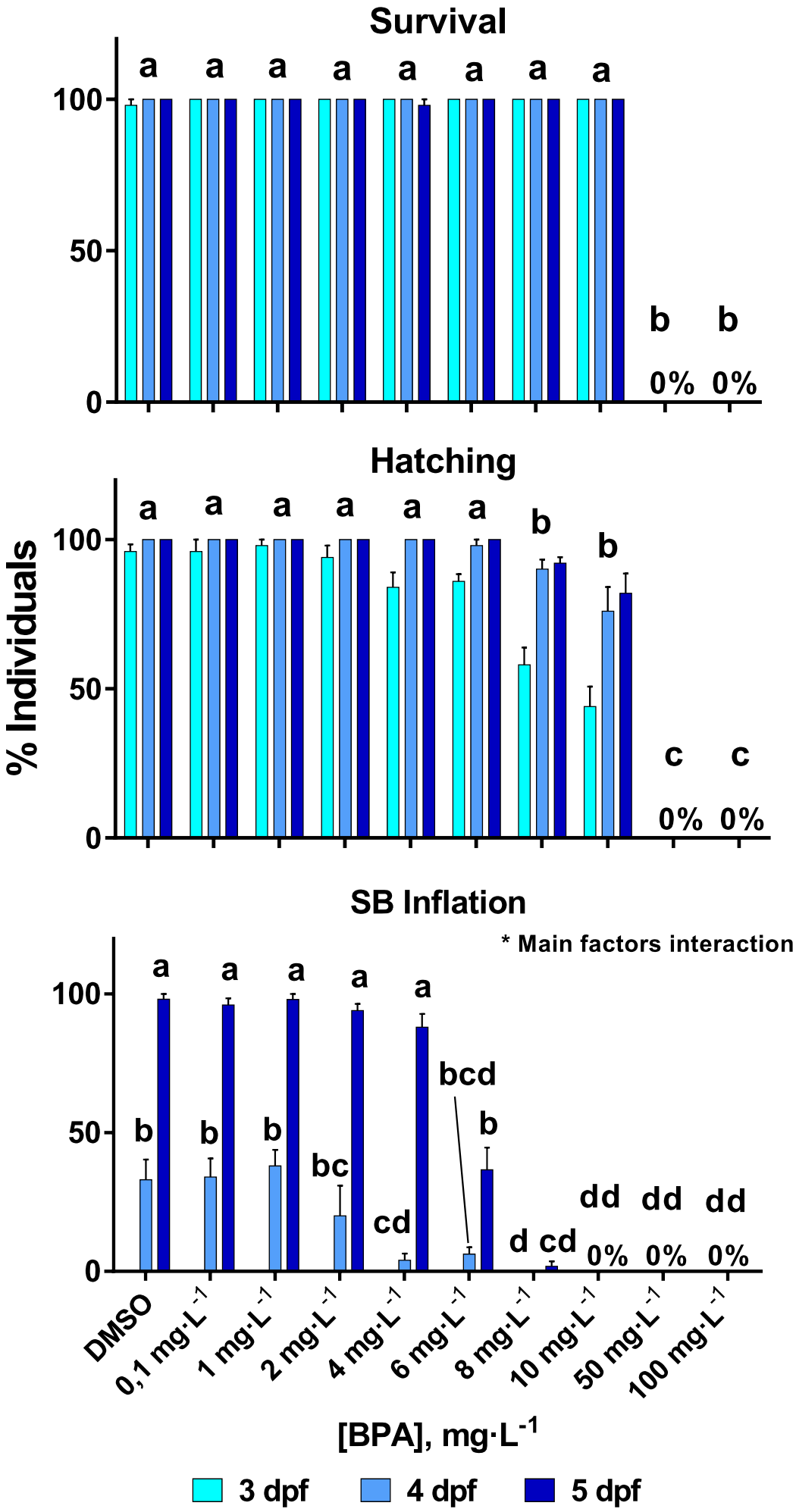

Supplementary Figure SF1

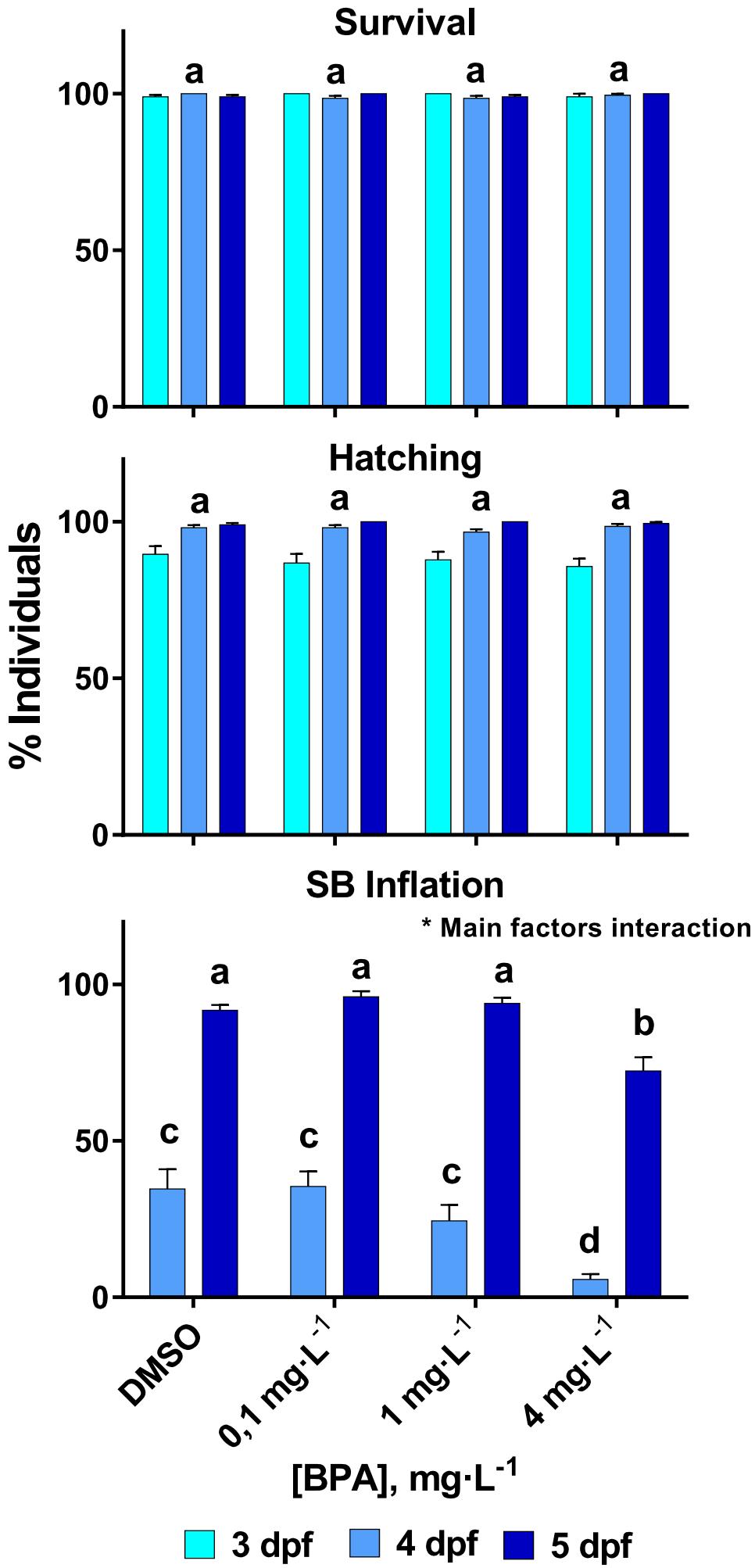

Supplementary Figure SF2

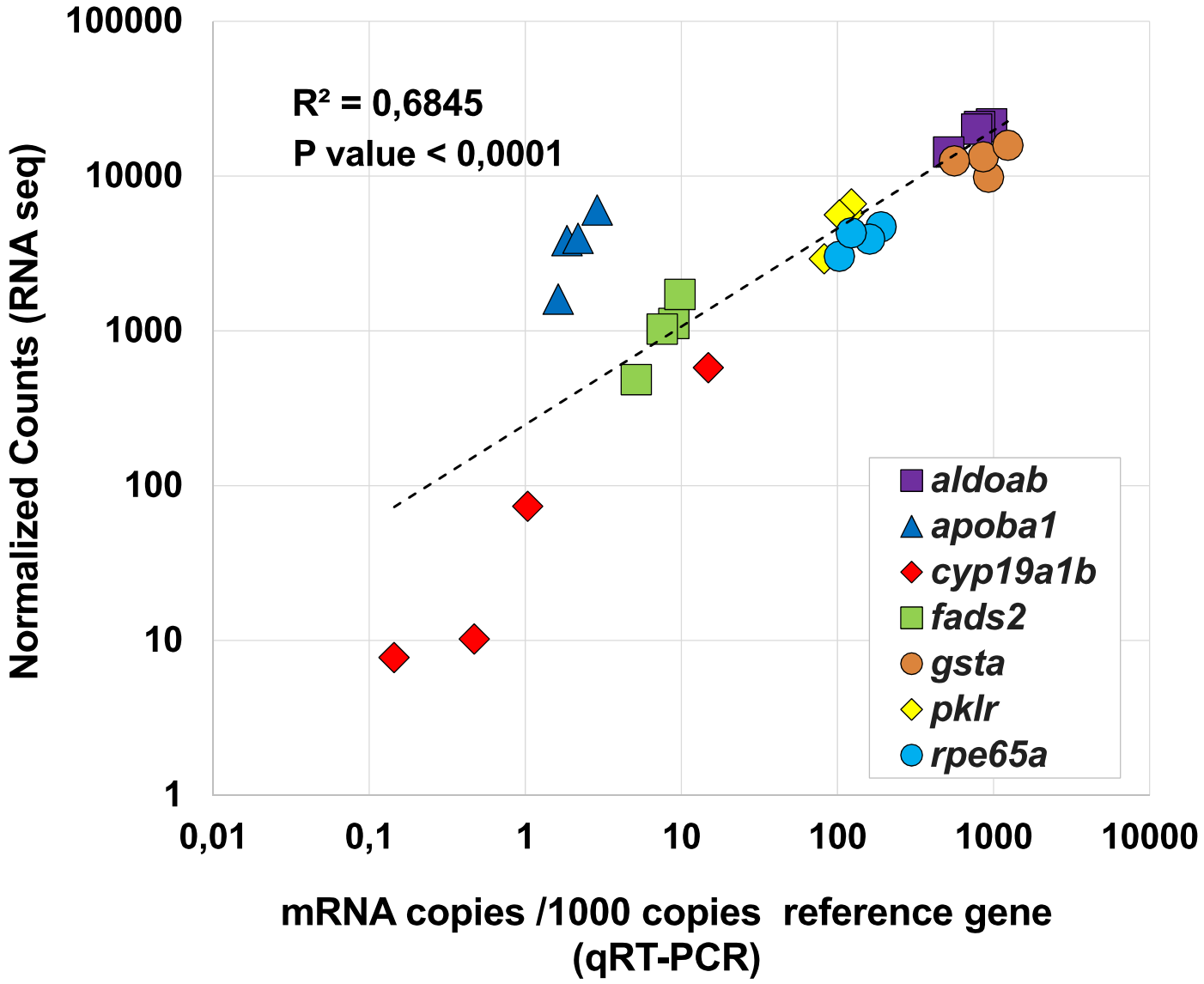

Supplementary Figure SF3

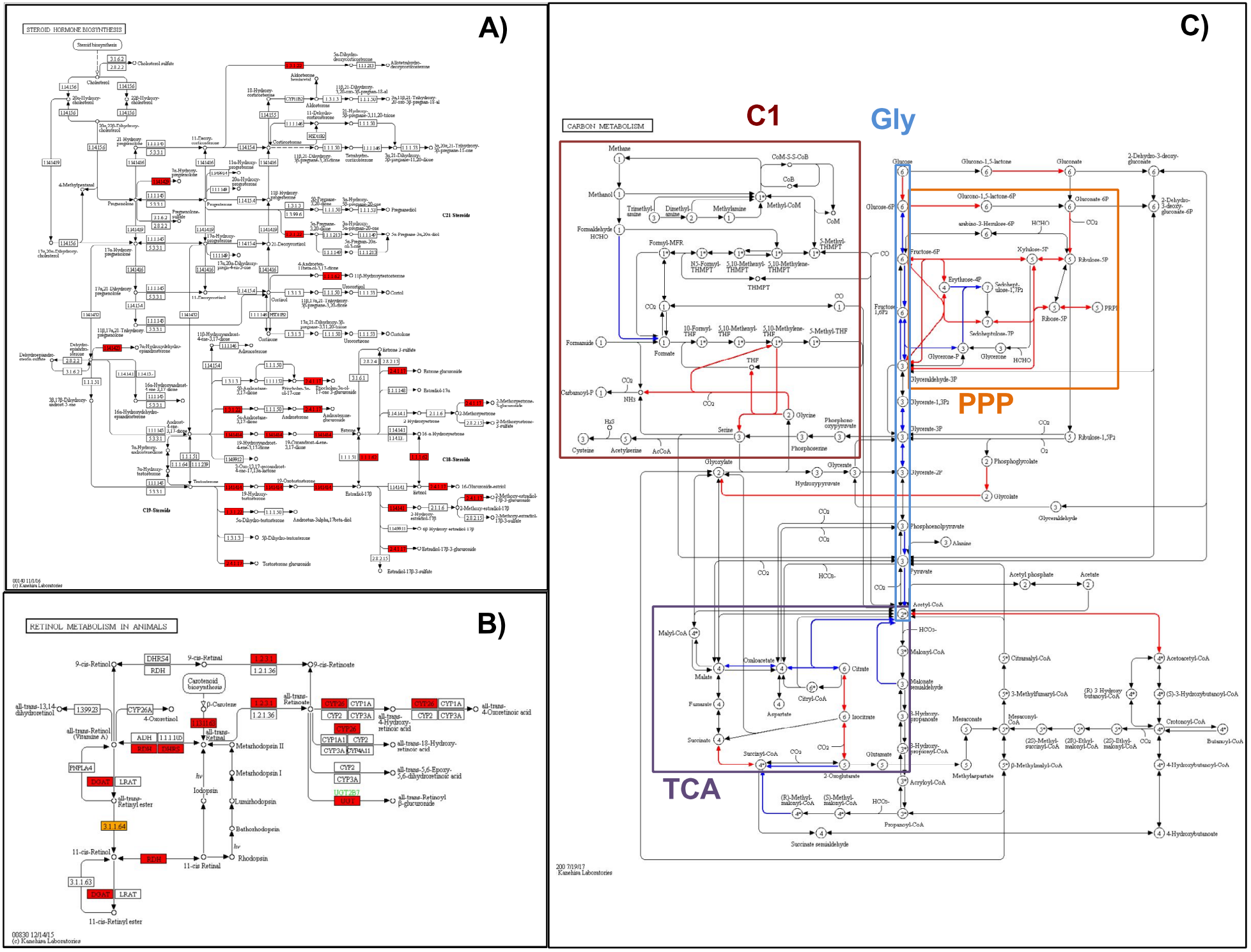

Supplementary Figure SF4

Supplementary Figure legends

Supplementary Figure 1. Survival, hatching and swim bladder (SB) inflation rates at 3, 4 and 5 dpf for the preliminary range finding test. Letters indicate statistically different sets of values (non-parametric Kruskal-Wallis test with pairwise multiple comparisons, $p < 0.05$). From these data, we derived a BPA concentration of 4 $mg \cdot L^{-1}$ as the macroscopic LOEC (lowest observed effect concentration). Survival rates at 50 and 100 $mg \cdot L^{-1}$ were 0% (displayed in the figure).

Supplementary Figure 2. Survival, hatching and swim bladder (SB) inflation results at 3, 4 and 5 dpf for the second experiment used for the transcriptomic analysis (control, 0.1, 1 and 4 $mg \cdot L^{-1}$ of BPA). Non-parametric test (Kruskal-Wallis test with pairwise multiple comparisons, $p < 0.05$) was performed. Letters indicate statistically different sets of values. LOEC value obtained (4 $mg \cdot L^{-1}$) is coincident with the preliminary range finding test results.

Supplementary Figure 3. Correlation between the results of RNA-seq and real-time qRT-PCR in the relative expression of 7 genes (aldoab, apoba1, cyp19a1b, fads2, gsta.1, pklr and rpe65a). The relative expression values obtained by RNA-seq and qRT-PCR are represented in y- and x-axis, respectively. A linear regression over the log-transformed values show a very strong correlation between the two quantitation methods ($p < 0.0001$, $R^2 = 0.6845$).

Supplementary Figure SF4. KEGG metabolic maps corresponding to modules dre00140 (Steroid hormone biosynthesis, **A**), dre00830 (Retinol metabolism, **B**) or dre01200 (Carbon metabolism, **C**). DEGs are cluster-colored in blue (Cluster A) or red (Cluster B). Glycolytic pathway (Gly, blue), pentose phosphate cycle (PPP, orange), C1 metabolism (C1, brown) and Krebs' cycle (TCA, purple) are highlighted in panel C.

Supplementary Table ST1. RNA-seq readings and mapping quality statistics.

Supplementary Table ST2. Results from DAVID Functional Analysis, FDR≤5%.

Supplementary Table ST3. Primers, efficiency and accession number for the genes measured with qRT-PCR (*ppiaa, aldoab, apoba1, cyp19a1b, fads2, gsta.1, pklr,* and *rpe65a*).